This document is the accepted manuscript version of the following article:
Vitali, V., Klesse, S., Weigt, R., Treydte, K., Frank, D., Saurer, M., & Siegwolf, R. T. W. (2021). High-frequency stable isotope signals in uneven-aged forests as proxy for physiological responses to climate in Central Europe. Tree Physiology, 41(11), 2046-2062. https://doi.org/10.1093/treephys/tpab062

High-frequency stable isotope signals in uneven-aged forests as proxy for physiological responses to climate in Central Europe

Short title: High-frequency isotope variations in tree rings

Valentina Vitali[1], Stefan Klesse[2,5], Rosemarie Weigt[1, 3], Kerstin Treydte[1], David Frank[1,4], Matthias Saurer[1,3], Rolf T.W. Siegwolf[1,3]

[1] Swiss Federal Institute for Forest, Snow and Landscape Research WSL, Forest Dynamics, CH-8903 Birmensdorf, Switzerland

[2] Swiss Federal Institute for Forest, Snow and Landscape Research WSL, Swiss Forest Protection, CH-8903 Birmensdorf, Switzerland

[3] Paul Scherrer Institute, Ecosystem Fluxes Group, Laboratory of Atmospheric Chemistry, CH-5232 Villigen PSI, Switzerland

[4]University of Arizona, Laboratory of Tree-Ring Research, Tucson, AZ, USA

[5]Swiss Federal Institute for Forest, Snow and Landscape Research WSL, Forest Resources and Management, CH-8903 Birmensdorf, Switzerland

Abstract

Picea abies and *Fagus sylvatica* are important tree species in Europe, and the foreseen increase in temperature and VPD could increase the vulnerability of these species. However, their physiological

performance under climate change at temperate and productive sites is not yet fully understood, especially in uneven aged stands.

Therefore, we investigated tree-ring width and stable isotope chronologies ($\delta^{13}C/\delta^{18}O$) of these two species at ten sites along a climate gradient in Central Europe. In these uneven-aged stands, we compared the year-to-year variability of dominant and suppressed trees for the last 80 years in relation to the sites' spatial distribution and climate.

$\delta^{18}O$ and $\delta^{13}C$ were generally consistent across sites and species, showing high sensitivity to summer VPD, whereas climate correlations with radial growth varied much more and depended on mean local climate. We found no significant differences between dominant and suppressed trees in the response of stable isotope ratios to climate variability, especially within the annual high-frequency signals. Additionally, we observed a strikingly high coherence of the high-frequency $\delta^{18}O$ variations across long distances with significant correlations above 1500 km, while the spatial agreement of $\delta^{13}C$ variations was weaker (~700 km). We applied a dual-isotope approach that is based on known theoretical understanding of isotope fractionations to translate the observed changes into physiological components, mainly photosynthetic assimilation rate and stomatal conductance. When separating the chronologies in two time windows and investigating the shifts in isotopes ratios, a significant enrichment of either or both isotope ratios over the last decades can be observed. These results, translated by the dual-isotope approach, indicate a general climate-driven decrease in stomatal conductance. This improved understanding of the physiological mechanisms controlling the short-term variation of the isotopic signature will help to define the performance of these tree species under future climate.

Keywords: *Fagus sylvatica, Picea abies*, stand dynamics, stable isotopes, tree ring, drought, climate change.

1 Introduction

The sensitivity of forest growth and physiological response to climate change and increasing atmospheric CO_2 is highly variable between tree species and ecosystems of different climatic regions (Lindner et al. 2010). Nevertheless in Central Europe increasing temperature and drought events' frequency and intensity have resulted in major productivity losses (IPCC 2019). Temperature increase and high vapour pressure deficit (VPD) have been identified globally as major tree stressors (Ficklin and Novick 2017; Grossiord et al. 2020), leading to both changes in transpiration demand and depletion of soil moisture (Eamus et al. 2008; Williams et al. 2013), with associated enhanced tree mortality (Adams et al. 2010; McDowell et al. 2011a; Will et al. 2013). However, growth is also limited by too high/low temperatures, nutrient availability, and further influenced by management or competition (Duquesnay et al. 1998; Peñuelas et al. 2008; Andreu-Hayles et al. 2011; Gómez-Guerrero et al. 2013; Rezaie et al. 2018). The interaction of all these factors leads to large uncertainties in the understanding of trees' physiological mechanisms, and adaptation potentials.

Tree rings have been widely used as proxies to assess the effect of climate variables on tree growth (Schweingruber 1976) and to understand the biological responses to environmental variability. Tree rings not only provide a unique source of information on annual radial increment, but store carbon and oxygen isotopes in the cellulose molecules ($\delta^{13}C$ and $\delta^{18}O$) providing time-accurate information on tree physiological processes modulated by climatic and site conditions (McCarroll and Loader 2004; Saurer et al. 2014). However, our understanding of the effects of climate change on tree physiological responses along temperate forests' climate gradients is still limited, as these effects are often studied at the edge of species ecological distribution, where growth rates are controlled by single factors, being it temperature (e.g. tree line sites (Friedrichs et al. 2009) or water availability (Büntgen et al. 2010)).

Differences of year-to-year variability and climate sensitivity between canopy layers in uneven-aged temperate forests have been hardly investigated, although the understanding of dominant and suppressed trees responses is necessary to fully understand forest functioning (Buchmann et al. 1997; Labuhn et al. 2014; Klesse et al. 2018). It is known that in a multi-layered forest the wood and leaf $\delta^{13}C$ signatures of the different strata are a product of light availability effects on photosynthetic potential (Buchmann et al. 1997), VPD canopy gradients (Barbour et al. 2004), $\delta^{13}C$-depleted CO_2

from the forest floor respiration (Bowling et al. 2005), and decline in stomatal conductance with increasing tree height (McDowell et al. 2011b). Further, the $\delta^{18}O$ ratios are affected by root system development and consequent access to deeper soil water (depleted in ^{18}O) vs surface soil water (enriched in ^{18}O through evaporation) (Roden et al. 2000). However, it is still largely unknown how these microclimatic factors influence the high-frequency information, intended as inter-annual or year-to-year variation of $\delta^{13}C$ and $\delta^{18}O$, recorded in tree rings.

High-frequency chronologies of TRW, $\delta^{13}C$ and $\delta^{18}O$ can be a source of important information, after long-term trends caused by ageing, height growth and stand development (Brienen et al. 2017; Klesse et al. 2018) have been removed. They retain only the year-to-year variation of growth or isotope ratios, providing insight into species' reaction and sensitivity to short-term climate variability. Increased $\delta^{13}C$ values of tree rings are directly connected to water stress, as it induces stomatal closure and lower leaf-internal CO_2-concentration, leading to poorer discrimination against the heavier ^{13}C (Farquhar et al. 1989). $\delta^{18}O$ signatures are indicators of large-scale hydrological processes and transpiration rates (McCarroll and Loader 2004), as they can be affected by source water, air water vapour, and mixing of evaporated and unevaporated water signals during sugar and cellulose formation (Roden et al. 2000). Nonetheless, $\delta^{18}O$ values of tree rings have proven their potential as strong climate proxy (Treydte et al. 2006; Treydte et al. 2007; Rinne et al. 2013; Labuhn et al. 2016), as precipitation and source water isotope signatures are related to temperature, and leaf water enrichment is VPD-dependent, imprinting the climate signal in plant biomass (O'Reilly Sternberg 2009) after known fractionation processes are accounted for (Gessler et al. 2014; Treydte et al. 2014; Lehmann et al. 2017).

The isotopic variations recorded in tree-ring cellulose in temperate and mesic sites can hold a stronger climate signal than tree-ring width, allowing for larger-scale synchronicity, with the potential to extend climate reconstructions from extreme to more temperate regions (Treydte et al. 2007; Hartl-Meier et al. 2015), and improve our mechanistic understanding of physiological responses to climatic changes (Scheidegger et al. 2000; Maxwell et al. 2020). Despite a broader inter-annual variability in growth rates at temperate sites than at the edge of species' distribution (Schweingruber 1976), consistent changes in physiological performance due to environmental conditions can still be retrieved

from $\delta^{13}C$ and $\delta^{18}O$ of tree rings (Saurer et al. 1997; Schleser et al. 1999; Loader et al. 2007). Some examples of transect studies have shown generally good agreement among different $\delta^{13}C$ chronologies along altitudinal (Treydte et al. 2001), latitudinal (Arneth et al. 2002) gradients; and some provided a comparison between species and sites at European scale (Treydte et al. 2007) and in North America (Guerrieri et al. 2019; Levesque et al. 2019). Nonetheless, the consistency of inter-annual variability of $\delta^{13}C$ and $\delta^{18}O$ records at large scales, and their reliability in predicting climatic or physiological processes for economically important tree species requires further investigation.

Trees' adaptation of physiological mechanisms to environmental changes can be assessed by a combined analysis of tree rings $\delta^{13}C$ and $\delta^{18}O$ through the dual-isotope model (Scheidegger et al. 2000). This is important as our understanding of the effects and interactions of climate variables, CO_2 on stomatal conductance balance, net carbon assimilation and carbon use is far from being complete (Schleser et al. 1999; Gessler et al. 2014), especially when considering long time periods and large-scale networks. The conceptual model proposed by Scheidegger et al. (2000) provides a useful tool for the deduction of stomatal conductance (g_s) and average maximum net photosynthesis (A_{net}) dependent on these changes, and to disentangle the effects of forest stands' structural differences and along environmental gradients (Roden and Siegwolf 2012), both in natural and controlled conditions (Grams et al. 2007).

In Central Europe *Fagus sylvatica* [L.] (European beech) and *Picea abies* [L.] Karst. (Norway spruce) represent two of the most cultivated and thus economically important tree species. Both species are strongly impacted by climate change. Compared to spruce, beech has been shown to be less susceptible to summer droughts (Zang 2011; Pretzsch et al. 2013), however, sensitivity to drought periods have been recorded for both species in temperate forests of central Europe, especially in lower elevation forests, and is one of the major drivers of productivity and vitality losses in the last decade (van der Maaten 2012; Vitali et al. 2017; Schuldt et al. 2020). In this study, we investigated the information carried in the high-frequency tree-ring isotope variations of these two species, and applied the dual-isotope concept to a larger spatio-temporal scale to infer physiological responses of temperate forests to climate change. Klesse et al. (2018) showed that tree size dependent light attenuation in

dense forests can play a large role influencing long-term trends in $\delta^{13}C$ and $\delta^{18}O$ in European beech and Norway spruce. However, it remains unexplored whether year-to-year stable isotope ratio variability of trees from different canopy layers contains the same environmental information or not. We thus ask the following questions:

1. Which climate factors drive year-to-year variability of tree growth and isotope ratios of *Fagus sylvatica* and *Picea abies* across Central Europe, and how does the canopy position within the canopy influence the responses to environmental variation?
2. How consistent is the high-frequency signal of tree ring width, $\delta^{13}C$ and $\delta^{18}O$ chronologies between and within species at large scales?
3. How did climatic changes over the past century (1935-1973 compared to 1974 to 2013) affect relationships between $\delta^{13}C$ and $\delta^{18}O$, and what does this mean for tree physiological responses to climate at different crown levels?

2 Methods

2.1 Site and tree selection

We selected nine sites of a European tree-ring biomass network (presented in Keel et al. 2016, Keller et al. 2017 and Klesse et al. 2018; Fig. 1, Table1) with mostly uneven-aged stands dominated by spruce or beech, to ensure a wide range of tree sizes and ages. At all sites TRW, $\delta^{13}C$, and $\delta^{18}O$ measurements were performed on 10-13 trees, with the exception of the site SOR (Denmark) with only 7 trees and the sites RIF and PHD (Germany and Slovakia) with only 5 trees. Position of individual trees in the forest canopy is hereafter divided into two classes: dominant and suppressed, where the first class includes all top canopy trees (usually >20 m), while the second class consists of younger and smaller trees, creating two significantly different height groups. Further sampling and stand structure details can be found in Klesse et al. (2018) and chronologies statistics in Table S. 2. The sites encompass a gradient in temperature (ranging from 1°C to 11°C mean annual temperature) and precipitation (from 600 to 1700 mm total annual precipitation), and consequently a gradient in

summer VPD (2 -10 hPa) (Table1). For an easier interpretation of the results, it should be noted that the majority of the spruce sites are distributed towards higher elevations (between 1200-1966 m a.s.l.and one site at 430 m a.s.l.) than beech (between 35-1033 m a.s.l.), which corresponds to cooler and wetter conditions (Table 1, Fig.1). Only at the low-elevation site Riedenburg, Germany (hereafter RIF and RIP) both species are present. We used monthly mean temperature, precipitation totals, and vapour pressure from CRU TS4.03 (Harris et al. 2020) to calculate Standardized Precipitation Evapotranspiration Index (SPEI) with the R Package SPEI (Vicente-Serrano et al. 2010) using the Thornthwaite method. Monthly vapour pressure deficit (VPD) was calculated as:

$$VPD\ (hPa) = c_1^{\left(\frac{c_2 T}{c_3 + T}\right)} - Vap$$

where T is the average monthly temperature, Vap is the average monthly vapour pressure, c1−3 are constants with c1 = 6.1078, c2 = 17.08085 (at T > 0) or = 17.84362 (at T < 0), and c3 = 234.175 (T > 0) or = 245.425 (T < 0), according to Germany's National Meteorological Service (Deutscher Wetterdienst (DWD) 1979). Atmospheric CO_2 concentrations were derived from NOAA (http://www.esrl.noaa.gov/gmd) and McCarroll and Loader (2004).

2.2 Dendrochronological and tree-ring isotope analyses

Preparation of the tree cores for tree-ring width and stable isotope measurements followed standard procedures: a microtome cut was performed to obtain a plain surface suitable for TRW measurements. Ring widths were measured with TSAP-Win (Rinntech, Heidelberg) at 0.01 mm precision, cross-dated visually and with the software COFECHA (Holmes 1983), chronologies details are described in Table S. 2. Dated tree rings were cut with a scalpel under a binocular and analysed individually. Cellulose was extracted using Teflon bags (Ankom Technology, Macedon, NY, USA) following the Boettger et al. (2007) protocol, and further homogenized with a ultrasonic homogenizer (Laumer et al. 2009). Cellulose samples were packed into silver capsules through pyrolysis converted to CO_2 at 1450°C (PYROcube, Elementar, Hanau, Germany). Isotope ratios of carbon and oxygen were measured by mass spectrometry (IRMS) (Delta Plus XP; Thermo Finnigan Mat, Bremen, Germany) at a precision of ±0.15‰ for $\delta^{18}O$ and ±0.12‰ for $\delta^{13}C$. Values of $\delta^{13}C$ were further corrected as suggested by

(Woodley et al. 2012), and corrections for past changes of atmospheric CO_2 were also applied on the raw $\delta^{13}C$ data ($\delta^{13}C_{corr}$,hereafter $\delta^{13}C$) following (Leuenberger 2007; Belmecheri and Lavergne 2020). For further details of sample preparation we refer to Weigt et al. (2015) and Klesse et al. (2018).

2.3 Data analysis and statistics

While raw $\delta^{18}O$ and $\delta^{13}C$ data were used for application of the Scheidegger model (see below), first-order differenced (FDiff) TRW, $\delta^{13}C$ and $\delta^{18}O$ data were used to enhance the year-to-year variations for the climate correlation analysis. The FDiff data were calculated for each individual time series as the residuals of the tree-ring data of successive years to remove any long-term trends and lower frequencies.

We averaged the individual FDiff time series to site chronologies using Tukey's biweight robust mean. Accordingly, separate mean chronologies were constructed for the two canopy layers. Monthly climate data, also FDiff detrended, were used for correlation analysis, performed with the *treeclim* package (Zang and Biondi 2015). Climate correlations were calculated for the common period 1935-2013 and for two equally long time-windows 1935-1973 and 1974-2013, between which, either or both $\delta^{13}C$ and $\delta^{18}O$ showed significant changes (Fig. S.3). We used temperature (T), precipitation (P), vapour pressure deficit (VPD), and standardised precipitation-evapotranspiration index (SPEI) as climatic variables (Harris et al. 2020). All correlation analyses between tree-ring data and climate variables were calculated from the start of the previous growing season (i.e., previous February) to the end of the current year (current December), however, the June-July-August window yielded the highest correlations for all variables and was selected as the focus of our analyses. The first-differenced chronologies were used to test the correlations between sites and evaluate the signal degradation across increasing distances. Spatial correlation decay of the three tree-ring parameters within and between species was calculated using a negative exponential function.

To investigate the effect of canopy position and time period on the relationship between $\delta^{13}C$ FDiff and $\delta^{18}O$ FDiff (i.e., the regression slope) we applied linear mixed effects models per site defined as:

$$\delta^{13}C_i \sim \beta_0 + \beta_1\delta^{18}O_i + \beta_2\,\text{Canopy position}_i + \beta_3\text{Time period}_i +$$

$$\beta_4 \text{Time period}_i * \text{Canopy position} * \delta^{18}O_i + S_{0i} + S_{1i}\,\delta^{18}O_i + \varepsilon_i,$$

where the response variable is $\delta^{13}C$ FDiff for tree *i*, and the fixed effect variables are $\delta^{18}O$ FDiff (continuous), canopy position (two factors) and time period (two factors). β_0 to β_4 are the regression parameters to be estimated. S_0 denotes the random intercept (i.e. tree effect), and S_{1i} is the random slope for $\delta^{18}O$. FDiff. ε is the gaussian-distributed error. All computations were performed using R version 4.0.0 (R Core Team 2020) and the *lme4* package (Douglas Bates et al. 2015). Marginal (without random effects) and conditional (with random effects) r^2 were calculated with the help of the r.*squaredGLMM* function in the *MuMIn* package (Bartoń 2013). The significance of differences between regression slopes was calculated with the *lstrends* function from the package *lsmeans* (Lenth 2016).

2.5 Application of the Scheidegger model – recent changes of tree physiology

The dual isotope approach proposed by Scheidegger et al. (2000), relates changes in leaf level $\delta^{13}C$ and $\delta^{18}O$ to shifts in stomatal conductance (g_s) and photosynthetic rates (A_{net}) based on known isotope fractionation processes (Farquhar et al. 1989; Barbour et al. 2004). Beyond its original scope, this model can be applied to infer physiological changes from the shifts in the mean of the isotopic composition recorded in tree rings between two time periods, as illustrated in Fig. 2. In our case, we observed significant changes in $\delta^{18}O$ and $\delta^{13}C$ between the two time-windows (Fig.S.3), which suggests significant shifts in physiological mechanisms. The mean isotope values at T_0 (centre of the plot) represent the average for the time period 1935-1973 the T_1 values (i.e. for the 1974-2013 window) are at the end of one of the arrows. For example, increasing $\delta^{13}C$ and $\delta^{18}O$ values would indicate a decline in stomatal conductance over time (arrow n.2), while constant $\delta^{18}O$ but increasing $\delta^{13}C$ suggest an increase in photosynthesis but no change in stomatal conductance (arrow n.1).

Here, we evaluate not only the differences between sites regarding their temporal patterns, but we also evaluate how physiological changes differ between canopy classes, and relate those differences to the dominant environmental driver derived as described above. Due to the lack of source water time

series, we assume that the impact is constant between our time-windows, and further conclusions are to be considered with the limitation of the model in mind.

3 Results

3.1 Climate correlations

The FDiff $\delta^{13}C$ and $\delta^{18}O$ data showed very homogenous and strong responses to summer climate for both species, while FDiff TRW showed heterogeneous and weaker relationships. Both $\delta^{13}C$ and $\delta^{18}O$ variations of most sites were significantly ($P \leq 0.05$) and positively correlated with summer season FDiff temperature and VPD, and negatively with precipitation and SPEI (Fig. 3 a-h), without a clear species-specific or mean climate-dependent response pattern. These results were similar for both canopy layers.

In contrast to the stable isotope ratios, the climate correlations of TRW (Fig. 3 i-n) varied strongly across our sites and we found positive and negative correlations for both species. This reflects the site selection along a climatic gradient rather than sampling only at e.g., dry and warm sites where a similar climate signal could be expected for all sites. For example, tree growth at lower elevation and warmer sites was significantly negatively correlated with temperature and positively correlated with precipitation (CIM, RIE, RIP, SOR), while at the cooler and higher elevation sites we found negative correlations with precipitation and positive with temperature and VPD (DVN, N19, PGB, PHD). Both species shared the same climate signal, when growing at the same site (RIF and RIP).

To further investigate the temporal stability of the strong correlations FDiff $\delta^{13}C$, $\delta^{18}O$, and TRW to VPD we split the data into two equally long periods 1935-1973 and 1974-2012. Similar to the full period, climate correlations of the different periods and canopy layers did not systematically differ for the stable isotope ratios or TRW (Fig. 4). Climate correlations between the two periods were considerably stable for $\delta^{13}C$ and $\delta^{18}O$ and, in the majority of cases, an increase in the significance can be observed in the later period, except for FLA and RIF. On the contrary, TRW showed a general decrease of correlation values with summer VPD for the dominant trees in the later time period, and even a significant change in sign in the suppressed trees (e.g. from +0.2 to -0.3 in FLA). We further

investigated the relevance of these shifts between the time periods with the help of the dual-isotope model in section 3.4.

3.2 Spatial relationships

Across Europe, both $\delta^{13}C$ and $\delta^{18}O$ chronologies show much higher spatial correlations compared to TRW chronologies (Fig. 5). For all parameters, correlations showed a negative exponential decline with distance between sites. The FDiff TRW chronologies showed high variability at any given distance and the weakest overall site-to-site correlations. Even at short distances (300 km) we observed pairs of sites with either especially high ($r^{2=}$0.6 DAV-N19) or especially low (r^2=-0.2 DAV-RIP) correlations (Fig. 5 a). $\delta^{13}C$ correlations showed a strong decline with increasing distance, becoming insignificant (r^2<0.25) at a distance of >1000 km. $\delta^{18}O$ correlations showed the highest and most consistent synchronization between sites, even at large distances (>1500km). In particular, the two beech sites in Germany and Switzerland (FLA- RIF, both low elevation) and spruce in Switzerland (DVN-N19, both high elevation), showed very high correlations, even at a distance of ~500 km, with values of r=0.79 and r=0.83 respectively. Correlations between these two site pairs were also very high for $\delta^{13}C$ chronologies (r=0.71, r=0.62), while their TRW correlations were lower (0.34 and 0.60, respectively). However, also site pairs with very different elevations and with two different species showed high correlations, e.g. DAV-FLA with an elevation difference of ~1000m (1600 vs 600 m a.s.l.), where $\delta^{18}O$ (r=0.80), $\delta^{13}C$ (r=0.49), and also TRW (r=0.33) were significantly correlated. Interestingly, the inter-specific correlations were not different from the intra-specific correlations. Inter-specific correlations appeared to be lower for TRW compared to intra-specific correlations, whereas differences between spatial correlation patterns for $\delta^{13}C$ and $\delta^{18}O$ were very small for both species-specific correlations and for between-species correlations.

3.3 High frequency relationships between $\delta^{13}C$ and $\delta^{18}O$

High-frequency relationships between $\delta^{13}C$ and $\delta^{18}O$ were consistently positive across all sites and canopy layers for all time-windows although beech showed on average a steeper regression slope (0.32) compared to spruce (0.17), and on average a higher R^2. For both species conditional R^2 remained very similar to the marginal R^2 (Fig. 6), indicating little variability in the isotopic relationship between individual trees. On average, we found a 1 ‰ increase of $\delta^{18}O$ corresponds to only a 0.32‰ $\delta^{13}C$ change for beech and a 0.17‰ $\delta^{13}C$ change for spruce. In all cases, we did not

observe statistically significant differences between the two canopy layers in the same time period. However, we found significant but non-systematic differences between the two time periods at four sites: at two sites (N19 and FLA) the early period revealed stronger positive changes in $\delta^{13}C$ for a given change in $\delta^{18}O$, in case of N19 for both canopy layers, and in case of FLA for the dominant trees only (Fig. 6). At the other two sites (CUC and SOR) the second period revealed a steeper regression slope, but for the dominant trees only.

3.4 Dual isotope approach: Application of the conceptual Scheidegger model

When examining raw instead of FDiff mean tree-level $\delta^{13}C$ and $\delta^{18}O$ values, differences between sites and species become apparent, with higher $\delta^{13}C$ values for spruce compared to beech, and for dominant compared to suppressed trees (Fig. 7, Fig. S. 1). Considering the distribution of mean isotope ratios within each site (Fig. S. 2 a), $\delta^{18}O$ is more consistent compared to $\delta^{13}C$ with larger between-trees variability, also when comparing the two canopy layers, where $\delta^{13}C$ values of the dominant trees were most variable. All sites and both canopy layers showed a similar positive relationship between mean tree-level $\delta^{13}C$ and $\delta^{18}O$ (Fig. S. 2 b), except for the suppressed beech trees at the RIF site, which showed a negative one.

Both species and both canopy layers showed strong temporal changes of mean site-level $\delta^{13}C$ and $\delta^{18}O$ values between time periods (Fig. 7, Table S. 3). In all cases the derived physiological scenarios responses indicate an unchanged or reduced stomatal conductance. Dominant trees represent three out of eight possible Scheidegger model scenarios, suppressed trees showed a slightly more variable response, where three to four out of eight scenarios were found.

When $\delta^{18}O$ of dominant trees did not change significantly between the two time periods (PHD, PGB, CUC), $\delta^{13}C$ showed an increase (scenario 1). This can be explained by an increase in A, with constant g_s. In all other sites, but DAV, we interpret a simultaneous increase in $\delta^{13}C$ and $\delta^{18}O$ (scenario2) as a decrease in g_s, but not in A. The DAV site (scenario 3) was the only site where we see a decrease in both A and g_s.

We observed a similar pattern for the supressed trees. Two sites (N19, PGB) showed much stronger increases in $\delta^{13}C$ (scenario 1), suggesting an increase in A relative to unchanged g_s. At three sites we found a simultaneous increase in $\delta^{13}C$ and $\delta^{18}O$ (FLA, CIM, CUC) (scenario 2), hinting at a decreased stomatal conductance over time. A slight decrease in mean $\delta^{13}C$ with simultaneous increase in $\delta^{18}O$ (scenarios 3 and 4) at DAV and RIF can be interpreted as decrease in both A and g_s over time, potentially with stronger reductions in A relative to g_s.

4 Discussion

This study highlights that the inter-annual variability of stable isotope ratios carries the same climatic signal independent of the tree's position in the canopy layer. We further showed the large spatial synchrony of $\delta^{18}O$ high frequency signals across Central Europe, and identified summer VPD as the major climatic driver of the high frequency tree-ring isotopic signatures. Interestingly, we did not find distinct species-specific differences, besides spruce showing overall higher raw $\delta^{13}C$ values, flatter high-frequency relationships and lower correlations between the two isotope ratios compared to beech. In addition, suppressed trees showed consistently lower $\delta^{13}C$ values than dominant trees regardless of the species. Finally, the impact of changing climatic conditions, i.e. warmer and drier summers, predominantly indicated a decrease of stomatal conductance at all sites over time. Hereafter we discuss the physiological mechanisms driving these responses.

4.1 Consistent impact of summer climate on isotopic composition

Regardless of site location we found vapour pressure deficit (VPD) of the summer months June to August to be the strongest climate driver of both stable isotope ratios (Fig. 3 and 4), although SPEI of the same months was only slightly less correlated. The high sensitivity of $\delta^{18}O$ to summer drought has been observed in other studies (Treydte et al. 2007; Labuhn et al. 2016; Levesque et al. 2017; Loader et al. 2020), where $\delta^{18}O$ variability was attributed also to variation in source water and precipitation (Treydte et al. 2006; Saurer et al. 2012; Weigt et al. 2018). Also, the strong correlation of $\delta^{13}C$ to summer drought variability - either represented by precipitation, water availability or cloud cover - has

been previously reported (Saurer et al. 1995; Gagen et al. 2006; Andreu et al. 2008; Kirdyanov et al. 2008; Mölder et al. 2011; Gagen et al. 2011; Hartl-Meier et al. 2015; Schäfer et al. 2017).

The strong response to VPD is consistent with the generally good correlation between the year-to year differences in $\delta^{13}C$ and $\delta^{18}O$ across most sites (Fig. 4). This result was independent of the trees' position within the canopy and emphasizes the role of stomatal conductance in controlling leaf gas exchange and their strong dependency on atmospheric moisture conditions (Saurer et al. 2008; Hartl-Meier et al. 2015; Salmon et al. 2020). Similar isotopic covariance has been reported for a combination of species and sites in temperate forests across Europe (Treydte et al. 2007), for *Pinus sylvestris* in Sweden (Esper et al. 2018), and *Larix decidua* in Switzerland (Weigt et al. 2018), for multiple species across the northeastern US (Guerrieri et al. 2017), in semi-arid conifers in the southwestern U.S. (Szejner et al. 2016) and mesic conifer forests in China (Liu et al. 2014). However, correlations focusing specifically on high-frequency signals in $\delta^{13}C$ and $\delta^{18}O$ are rarely investigated.

A precipitation signal recorded in tree-ring's $\delta^{13}C$ and $\delta^{18}O$ that is independent of mean climate and species, challenges the assumption that locally drier sites record the clearest precipitation signal (Saurer et al. 1995; McCarroll and Loader 2004). However, it is consistent with the finding that isotope ratios are also sensitive to climate and soil water availability on temperate sites (Hartl-Meier et al. 2015), or precipitation and VPD in mesic sites (Levesque et al. 2017). Concurrently, numerous factors (e.g. species-specific differences) influence isotope fractionation and tree-ring formation making the relationship between tree growth and $\delta^{13}C$ not always straightforward (Gessler et al. 2014). Contrary to the stable isotope ratios and as expected, TRW sensitivity to summer drought was overall much weaker at these temperate sites and only significant at the driest and warmest sites (RIF, RIP and CIM). Similar findings were also reported in other studies where the correlations between TRW and the climate variables were inconsistent compared to the isotopes correlations (e.g. (Andreu et al. 2008; Hartl-Meier et al. 2015)). The similar climate sensitivity of beech and spruce is also surprising considering their responses to recently increased droughts in Europe, where high vulnerability and mortality events of spruce were reported (Vitali et al. 2017; Vitasse et al. 2019; Bosela et al. 2020; Krejza et al. 2020; Schuldt et al. 2020) and forest models predict strong reduction in the distribution of

spruce at low elevations in coming decades (Hanewinkel et al. 2013; Kolář et al. 2017). Nevertheless, beech was also shown to be more susceptible to drought than previously assumed (Löw et al. 2006; Gessler et al. 2006; Piovesan et al. 2008; Walthert et al. 2020).

Recent research has been focusing on the impact of increasing VPD from the leaf to the global scale, and on its effects on plant physiology (Breshears et al. 2013; Grossiord et al. 2020). Numerous studies, both in natural (Liu et al. 2008; van Mantgem et al. 2009; Allen et al. 2010; Allison 2011) and controlled experiments (McDowell et al. 2011a) reached the main conclusion that the impact of VPD is a strong trigger of metabolic feedbacks, potentially exacerbating precarious situations, when in concomitance with drought events. VPD as a major tree stressor, can lead to changes in tree physiology (Eamus et al. 2008), affecting phloem functions, increasing xylem tensions (Adams et al. 2010; McDowell et al. 2011a), and the impact of climate-change induced VPD increase (Held and Soden 2006; Ficklin and Novick 2017; IPCC 2019) could lead to loss in vitality and major mortality events (Breshears et al. 2013).

The strong signal recorded in our chronologies suggests that summer VPD at our sites is strongly regulating trees' transpiration, stomatal conductance, and photosynthesis. The strong response implies an active metabolic system currently still able to cope with varying water availability at these sites. However, this could drastically change if increasing temperatures and atmospheric evaporative demand hinder photosynthesis, driving loss in primary productivity and amplifying drought susceptibility.

4.2 Long distance coherence of high frequency isotope chronologies

The inter-annual variability of $\delta^{13}C$ and $\delta^{18}O$ chronologies (FDiff) showed remarkably high correlations between sites that are hundreds of km apart, independent of local mean climate (Fig. 5). This is in contrast to much lower correlations between the TRW chronologies, even across short distances. In particular, $\delta^{18}O$ records show a remarkable coherence, with correlations up to r=0.8 between sites that are 600km apart, and only at a distance of about 1500 km, correlation values decrease to r=0.3, which corresponds to the average site-to-site correlation value for TRW in this

network. $\delta^{13}C$ shows a steeper decline than $\delta^{18}O$ with increasing site distances, however it still performed better (mean r=0.6) than TRW in the first 1000km between sites. Considering the scale of this transect and that this comparison includes an evergreen conifer and a deciduous broadleaved species, this high degree of uniformity is striking. The low correlations between TRW chronologies are also partially explained by the site selection, which was not designed to maximize coherence and climate signals in TRW avoiding extreme sites at e.g. the dry and warm edge, and rather focusing on temperate sites along a climatic gradient. Our results underline previous findings that the limiting environmental factors driving TRW variability may change on small scales and strongly depend on mean climate conditions, such as mean annual precipitation sums, mean annual temperature and their combination (Klesse et al. 2020). Contrary to TRW the main limiting factor controlling year-to-year variability in $\delta^{13}C$ and $\delta^{18}O$ (i.e. summer VPD) seems to be much less influenced by local mean climate. This can explain the much stronger and larger spatial coherence between our stable isotope chronologies compared to the TRW chronologies. The spatial fingerprint of high correlations mirrors the extent of the main climatic region, in our case central European climate dominated by westerlies. This is why the correlation points including CIM (central Italy) are predominantly lower compared to the rest, because the site is situated in a different main climatic regime (Mediterranean, Fig. 5 b and c).

Similarly, on a larger scale Treydte et al. (2007) showed regional patterns of high synchronicity across Europe, with different light-demanding genera (*Pinus, Quercus, Cedrus*), which also showed a larger-range reliability of $\delta^{18}O$ compared to $\delta^{13}C$. Further analyses on TRW and $\Delta^{13}C$ on the Treydte et al. (2007) dataset highlighted an increased growth synchrony across European forests, although not uniformly, due to warming-induced effects of drought on leaf physiology (Shestakova et al. 2019). Hartl-Meier et al. (2015) emphasized high uniformity of climate sensitivity for both $\delta^{13}C$ and $\delta^{18}O$ in European beech and Norway spruce (as well as European larch) at temperate sites, although at shorter distances. Our study combines and extends results of such studies, merging the long-range correlations and the comparison of evergreen conifer and a deciduous broadleaved species, providing further evidence of the large-range synchrony of high frequency isotopic signals.

4.3 Interpretation of physiological responses

When considering the raw isotope data, substantial differences in the range of values of the isotopic signatures with offsets up to ~6‰ for $\delta^{13}C$ and $\delta^{18}O$ for both species were found. Spruce generally showed higher $\delta^{13}C$ values and within a smaller range than beech, even when growing at the same site (RIP, RIF), indicating lower stomatal conductance of the conifer species as compared to broadleaf beech. Beech $\delta^{13}C$ values were significantly more depleted than spruce, reflecting higher discrimination of ^{13}C from higher stomatal conductance and/or a lower photosynthetic rate, and hence, lower intrinsic water use efficiency (Leavitt 1993; Lévesque et al. 2013). These differences underline the less isohydric behaviour of beech compared to spruce (Klein 2014), i.e. higher stomatal conductance, lower leaf water potentials and higher root capacity for soil exploration and access to deeper soil water pools than spruce, especially under drought (Pretzsch et al. 2013).

The larger variability of beech's raw $\delta^{18}O$ records compared to spruce (Fig. 6) can be attributed to the differences in sites conditions (Fig. S. 1), the difference in the rooting depth of the two species and the large climatic range of beech species. It is known that, compared to deep soil water, surface soil water is enriched in ^{18}O through evaporation (Roden et al. 2000). Therefore, the shallow rooting system typical of spruce restricts its access to surface water, and consequently will be more enriched in ^{18}O (Boratyński et al. 2007), compared to deep rooting beech, which can show depleted ^{18}O values, depending on water uptake (Treydte et al. 2007; Balting et al. 2020) . This can also explain the larger $\delta^{18}O$ variability of beech at our sites (Fig. 6), as they range between wetter sites, where $\delta^{18}O$ is sourced at shallower depths, and therefore more enriched; to drier sites, where beech has access to deeper water resources, resulting in more depleted and consistent values (Volkmann et al. 2016) (Fig. S. 1). However, when comparing different time periods, we assume changes in rooting depth at single sites to be negligible and resulting changes in $\delta^{18}O$ to be due to tree physiological changes.

For trees of the dominant group, we did not expect a change in canopy position over the last 80 years, either. Thus, we interpret that the shifts in $\delta^{18}O$ and $\delta^{13}C$ reliably record changes in the species-specific physiological responses to changing climate. We showed that the position in the canopy and age appear to have only small effects on the inter-annual variability of isotopic ratios. Together with recent findings that tree size trends play a minor role on discrimination once trees approach their maximum

height or are fully exposed to sunlight (Klesse et al. 2018), inferences formulated from datasets predominantly based from dominant trees can be extrapolated to the stand level of uneven-aged forests.

The conceptual model of Scheidegger et al. (2000) provides the means for deducing changes in g_s and A_{net} through examining the isotopic shifts in tree-ring cellulose through time, although it should be kept in mind that it is only a semi-quantitative model (Roden & Siegwolf, 2012). It allows to interpret our dual-isotope results assuming that changes in $\delta^{18}O$ are primarily driven by changes in leaf water enrichment caused by variation in air humidity, and changes in $\delta^{13}C$ by shifts in stomatal conductance responses to evaporative demand, and consequent lower plant water-use efficiency and photosynthesis. We found a strong positive temporal relationship between $\delta^{13}C$ and $\delta^{18}O$ for both dominant and suppressed trees, and deduced from the conceptual model that tree physiological rates (i.e. stomatal conductance and photosynthetic rate) have changed significantly over the past century, primarily due to warmer summer temperatures and the concomitant increase in VPD. In both canopy layers 60% of the sites showed a scenario 2 behaviour, where both $\delta^{13}C$ and $\delta^{18}O$ increase, which translates into rather constant A_{net} and declining g_s, and hence, increased iWUE (Soh et al. 2019), also supported by the high frequency results.

Differences in mean $\delta^{13}C$ values between the two canopies suggest a lower A_{net} in suppressed compared to dominant trees. The most likely explanation is increased light attenuation in smaller trees, leading to less efficient photosynthesis (Klesse et al. 2018). In three cases, (i.e. the suppressed trees at RIF and both canopy layers at DAV), we observed a different trajectory of stable isotope ratios over time showing a decrease in A_{net} (scenario 3 and 4). At RIF both canopy layers have the same age and started roughly at comparable $\delta^{13}C$ and $\delta^{18}O$ values (early period). However, the decrease in $\delta^{13}C$ together with both increases in $\delta^{18}O$ and a drastic decrease in radial growth increment (c.f. Klesse et al. 2018) nicely pictures how these trees have been outcompeted and over-shaded by surrounding, more competitive trees. The observed trajectory within the Scheidegger model thus clearly represents a decrease in photosynthesis, while simultaneously climate change induced decreased stomatal conductance (c.f. dominant trees at RIF).

In this study, no site recorded an increase in g_s, and similar results are shown in other natural forests experiments, which recorded an increase in A_{net} in an old-grown high altitude larch forest (Weigt et al. 2018). This is most likely due to the lower altitude and tendency of warmer and drier conditions experienced in the second time window at all sites. Even at our highest elevation spruce site N19, we observed a marked increase in $\delta^{18}O$ and a likely climate-driven reduction of stomatal conductance; most likely connected to isohydric behaviour of spruce during drought periods, in which complete stomatal closure occurs at higher xylem water potential (Lyr 1992; McDowell et al. 2008; Weigt et al. 2015).

5 Conclusions

This study brings forward our understanding of the physiology of two economically important tree species along a European transect, through the analyses of high-frequency patterns of climate sensitivity and concurrent isotope changes over time. High $\delta^{18}O$ coherence of the correlations of the year-to-year variability between species and strong dependence on VPD, independent of canopy layer, and across space highlight the strength of the environmental signal in the $\delta^{18}O$ chronologies, which paired with $\delta^{13}C$ supplements important climatological and physiological information. These results further prove the usefulness of stable isotope ratios as a tool for reconstructing past climatic conditions in mid-latitude, temperate environments especially when a strong climate signal is lacking in conventional tree-ring width or maximum latewood density.

Insight into differences and similarities between crown layers is important for a comprehensive assessment of forest ecosystem dynamics and carbon fluxes. On the one hand, our results suggest that all canopy layers should be included in ecological studies aimed at quantifying biomass or carbon sequestration rates, as structurally complex and mixed forests will hopefully become more frequent for climate change mitigation strategies (Dănescu et al. 2016; Vitali et al. 2018). Suppressed trees, which experience slow growing conditions in their juvenile stages, can slow down biomass turnover at the stand level and play a key role in enhancing CO_2 sequestration in the long-term (Büntgen et al. 2019), and carbon storage (Gray et al. 2016). Therefore, understanding their reactions to climate change creates a more complete picture of forest functioning. On the other hand, we show that there is little to

no difference in the high-frequency climate signal between trees of different ages and social classes, therefore a stratified canopy sampling is not strictly required to adequately capture interannual climate variation.

The dual isotopes approach indicated significant shifts in stomatal conductance at the majority of sites, when comparing two 40-year time-windows, which in concomitance with the high impact of summer VPD on all measured variables, indicates a trend of decreasing stomatal conductance across the whole transect. In light of climate projections increase in VPD, which could potentially exacerbate high vulnerability situations, especially in the dominant canopy layer, management actions focused on limiting the impact of climate change on forests, and mitigating strategies, such as mixed forest or uneven-aged stands to maintain forest cover, should be of high priority.

Funding and Acknowledgments

Thanks to all colleagues involved during the sampling campaign and especially to Olivier Bouriaud for providing the samples of the G2 plot, the LWF Bayern for allowing us to sample at their monitoring site RIE, Katarzyna Czober, Lenka Mateju, and Lola Schmid for their help in the laboratory. All authors (but VV) were supported by the SNF iTREE Sinergia Project 136295. VV is supported by SNF 200020_182092. SK acknowledges funding by the Federal Office for the Environment FOEN and the SwissForestLab Research Grant SFL-17 P3, and KT acknowledges support by the Swiss National Science foundation (SNF 200021_175888).

Authors' contributions

MS, RS were in charge of the project conceptualization, and methodology development. MS, KT, DF were the main supervisors, SK, RW were the main data producers and curators, VV wrote the original draft, analysis and visualization. All authors contributed to Reviewing and Editing.

6 Publication bibliography

Adams, Henry D.; Macalady, Alison K.; Breshears, David D.; Allen, Craig D.; Stephenson, Nathan L.; Saleska, Scott R. et al. (2010): Climate-Induced Tree Mortality: Earth System Consequences. In *Eos Trans. AGU* 91 (17), p. 153. DOI: 10.1029/2010EO170003.

Allen, Craig D.; Macalady, Alison K.; Chenchouni, Haroun; Bachelet, Dominique; McDowell, Nate; Vennetier, Michel et al. (2010): A global overview of drought and heat-induced tree mortality reveals emerging climate change risks for forests. In *Forest Ecology and Management* 259 (4), pp. 660–684. DOI: 10.1016/j.foreco.2009.09.001.

Allison, Ian (2011): The Copenhagen diagnosis. Updating the world on the latest climate science. Burlington MA: Elsevier.

Andreu, Laia; Planells, Octavi; Gutierrez, Emilia; Helle, Gerhard; Schleser, Gerhard H. (2008): Climatic significance of tree-ring width and δ13C in a Spanish pine forest network. In *Tellus B: Chemical and Physical Meteorology* 60 (5), pp. 771–781. DOI: 10.1111/j.1600-0889.2008.00370.x.

Andreu-Hayles, Laia; Planells, Octavi; Gutierrez, Emilia; Muntan, Elena; Helle, Gerhard; Anchukaitis, Kevin J.; Schleser, Gerhard H. (2011): Long tree-ring chronologies reveal 20th century increases in water-use efficiency but no enhancement of tree growth at five Iberian pine forests. In *Global Change Biol* 17 (6), pp. 2095–2112. DOI: 10.1111/j.1365-2486.2010.02373.x.

Arneth, A.; Lloyd, J.; Šantrůčková, H.; Bird, M.; Grigoryev, S.; Kalaschnikov, Y. N. et al. (2002): Response of central Siberian Scots pine to soil water deficit and long-term trends in atmospheric CO 2 concentration. In *Global Biogeochem. Cycles* 16 (1), 5-1-5-13. DOI: 10.1029/2000GB001374.

Balting, Daniel F.; Ionita, Monica; Wegmann, Martin; Helle, Gerhard; Schleser, Gerhard H.; Rimbu, Norel et al. (2020): Large scale climate signals of a European oxygen isotope network from tree-rings - predominantly caused by ENSO teleconnections? in review: Clim. Past Discuss.

Barbour, Margaret M.; Roden, John S.; Farquhar, Graham D.; Ehleringer, James R. (2004): Expressing leaf water and cellulose oxygen isotope ratios as enrichment above source water reveals evidence of a Péclet effect. In *Oecologia* 138 (3), pp. 426–435. DOI: 10.1007/s00442-003-1449-3.

Bartoń, Kamil (2013): MuMIn: Multi-model inference (1). In *R package version 1.10.0.*

Belmecheri, Soumaya; Lavergne, Aliénor (2020): Compiled records of atmospheric CO2 concentrations and stable carbon isotopes to reconstruct climate and derive plant ecophysiological indices from tree rings. In *Dendrochronologia* 63, p. 125748. DOI: 10.1016/j.dendro.2020.125748.

Boettger, Tatjana; Haupt, Marika; Knöller, Kay; Weise, Stephan M.; Waterhouse, John S.; Rinne, Katja T. et al. (2007): Wood cellulose preparation methods and mass spectrometric analyses of delta13C, delta18O, and nonexchangeable delta2H values in cellulose, sugar, and starch: an interlaboratory comparison. In *Analytical chemistry* 79 (12), pp. 4603–4612. DOI: 10.1021/ac0700023.

Boratyński, Adam; Bugała, Władysław; Tjoelker, Mark G. (2007): Biology and ecology of Norway spruce. Dordrecht: Springer (Forestry sciences, 78).

Bosela, Michal; Tumajer, Jan; Cienciala, Emil; Dobor, Laura; Kulla, Ladislav; Marčiš, Peter et al. (2020): Climate warming induced synchronous growth decline in Norway spruce populations across biogeographical gradients since 2000. In *Science of The Total Environment*, p. 141794. DOI: 10.1016/j.scitotenv.2020.141794.

Bowling, D. R.; Burns, S. P.; Conway, T. J.; Monson, R. K.; White, J. W. C. (2005): Extensive observations of CO 2 carbon isotope content in and above a high-elevation subalpine forest. In *Global Biogeochem. Cycles* 19 (3). DOI: 10.1029/2004GB002394.

Breshears, David D.; Adams, Henry D.; Eamus, Derek; McDowell, Nate G.; Law, Darin J.; Will, Rodney E. et al. (2013): The critical amplifying role of increasing atmospheric moisture demand on tree mortality and associated regional die-off. In *Frontiers in plant science* 4, p. 266. DOI: 10.3389/fpls.2013.00266.

Brienen, R. J. W.; Gloor, E.; Clerici, S.; Newton, R.; Arppe, L.; Boom, A. et al. (2017): Tree height strongly affects estimates of water-use efficiency responses to climate and CO2 using isotopes. In *Nature communications* 8 (1), p. 288. DOI: 10.1038/s41467-017-00225-z.

Buchmann, Nina; Kao, Wen-Yuan; Ehleringer, Jim (1997): Influence of stand structure on carbon-13 of vegetation, soils, and canopy air within deciduous and evergreen forests in Utah, United States. In *Oecologia* 110 (1), pp. 109–119. DOI: 10.1007/s004420050139.

Büntgen, Ulf; Brázdil, R.; Frank, David C.; Esper, Jan (2010): Three centuries of Slovakian drought dynamics. In *Clim Dyn* 35 (2-3), pp. 315–329. DOI: 10.1007/s00382-009-0563-2.

Büntgen, Ulf; Krusic, Paul J.; Piermattei, Alma; Coomes, David A.; Esper, Jan; Myglan, Vladimir S. et al. (2019): Limited capacity of tree growth to mitigate the global greenhouse effect under predicted warming. In *Nature communications* 10 (1), p. 2171. DOI: 10.1038/s41467-019-10174-4.

Dănescu, Adrian; Albrecht, Axel T.; Bauhus, Jürgen (2016): Structural diversity promotes productivity of mixed, uneven-aged forests in southwestern Germany. In *Oecologia* 182 (2), pp. 319–333. DOI: 10.1007/s00442-016-3623-4.

Douglas Bates; Martin Mächler; Ben Bolker; Steve Walker (2015): Fitting Linear Mixed-Effects Models Using lme4. In *Journal of Statistical Software* 67 (1), pp. 1–48. DOI: 10.18637/jss.v067.i01.

Duquesnay, A.; Breda, N.; Stievenard, Michel; Dupouey, J. L. (1998): Changes of tree-ring delta13C and water-use efficiency of beech (Fagus sylvatica L.) in north-eastern France during the past century. In *Plant Cell Environ* 21 (6), pp. 565–572. DOI: 10.1046/j.1365-3040.1998.00304.x.

Eamus, Derek; Taylor, Daniel T.; Macinnis-Ng, Catriona M. O.; Shanahan, Steve; Silva, Lionel de (2008): Comparing model predictions and experimental data for the response of stomatal conductance and guard cell turgor to manipulations of cuticular conductance, leaf-to-air vapour pressure difference and temperature: feedback mechanisms are able to account for all observations. In *Plant Cell Environ* 31 (3), pp. 269–277. DOI: 10.1111/j.1365-3040.2007.01771.x.

Esper, Jan; St. George, Scott; Anchukaitis, Kevin J.; D'Arrigo, Rosanne; Ljungqvist, Fredrik Charpentier; Luterbacher, Jürg et al. (2018): Large-scale, millennial-length temperature reconstructions from tree-rings. In *Dendrochronologia* 50, pp. 81–90. DOI: 10.1016/j.dendro.2018.06.001.

Farquhar, Graham D.; Hubick, K. T.; Condon, A. G.; Richards, R. A. (1989): Carbon Isotope Fractionation and Plant Water-Use Efficiency. In P. W. Rundel, James R. Ehleringer, K. A. Nagy (Eds.): Stable Isotopes in Ecological Research. New York, NY: Springer New York, pp. 21–40.

Ficklin, Darren L.; Novick, Kimberly A. (2017): Historic and projected changes in vapor pressure deficit suggest a continental-scale drying of the United States atmosphere. In *J. Geophys. Res. Atmos.* 122 (4), pp. 2061–2079. DOI: 10.1002/2016JD025855.

Friedrichs, Dagmar A.; Büntgen, Ulf; Frank, David C.; Esper, Jan; Neuwirth, Burkhard; Löffler, Jörg (2009): Complex climate controls on 20th century oak growth in Central-West Germany. In *Tree physiology* 29 (1), pp. 39–51. DOI: 10.1093/treephys/tpn003.

Gagen, M. H.; McCarroll, Danny; Edouard, Jean-Louis (2006): Combining Ring Width, Density and Stable Carbon Isotope Proxies to Enhance the Climate Signal in Tree-Rings: An Example from the Southern French Alps. In *Climatic Change* 78 (2-4), pp. 363–379. DOI: 10.1007/s10584-006-9097-3.

Gagen, M. H.; Zorita, Eduardo; McCarroll, Danny; Young, Giles H. F.; Grudd, Håkan; Jalkanen, Risto et al. (2011): Cloud response to summer temperatures in Fennoscandia over the last thousand years. In *Geophys. Res. Lett.* 38 (5), 1-5. DOI: 10.1029/2010GL046216.

Gessler, Arthur; Ferrio, Juan Pedro; Hommel, Robert; Treydte, Kerstin S.; Werner, Roland A.; Monson, Russell K. (2014): Stable isotopes in tree rings: towards a mechanistic understanding of isotope fractionation and mixing processes from the leaves to the wood. In *Tree physiology* 34 (8), pp. 796–818. DOI: 10.1093/treephys/tpu040.

Gessler, Arthur; Keitel, Claudia; Kreuzwieser, Jürgen; Matyssek, Rainer; Seiler, Wolfgang; Rennenberg, Heinz (2006): Potential risks for European beech (Fagus sylvatica L.) in a changing climate. In *Trees* 21 (1), pp. 1–11. DOI: 10.1007/s00468-006-0107-x.

Gómez-Guerrero, Armando; Silva, Lucas C. R.; Barrera-Reyes, Miguel; Kishchuk, Barbara; Velázquez-Martínez, Alejandro; Martínez-Trinidad, Tomás et al. (2013): Growth decline and divergent tree ring isotopic composition δ13C and δ18O contradict predictions of CO2 stimulation in high altitudinal forests. In *Global Change Biol* 19 (6), pp. 1748–1758. DOI: 10.1111/gcb.12170.

Grams, Thorsten E.E.; Kozovits, Alessandra R.; Häberle, Karl-Heinz; Matyssek, Rainer; Dawson, Todd E. (2007): Combining delta 13 C and delta 18 O analyses to unravel competition, CO2 and O3 effects on the physiological performance of different-aged trees. In *Plant Cell Environ* 30 (8), pp. 1023–1034. DOI: 10.1111/j.1365-3040.2007.01696.x.

Gray, Andrew N.; Whittier, Thomas R.; Harmon, Mark E. (2016): Carbon stocks and accumulation rates in Pacific Northwest forests: role of stand age, plant community, and productivity. In *Ecosphere* 7 (1). DOI: 10.1002/ecs2.1224.

Grossiord, Charlotte; Buckley, Thomas N.; Cernusak, Lucas A.; Novick, Kimberly A.; Poulter, Benjamin; Siegwolf, Rolf T.W. et al. (2020): Plant responses to rising vapor pressure deficit. In *The New phytologist*. DOI: 10.1111/nph.16485.

Guerrieri, Rossella; Belmecheri, Soumaya; Ollinger, Scott V.; Asbjornsen, Heidi; Jennings, Katie; Xiao, Jingfeng et al. (2019): Disentangling the role of photosynthesis and stomatal conductance on rising forest water-use efficiency. In *Proceedings of the National Academy of Sciences of the United States of America* 116 (34), pp. 16909–16914. DOI: 10.1073/pnas.1905912116.

Guerrieri, Rossella; Jennings, Katie; Belmecheri, Soumaya; Asbjornsen, Heidi; Ollinger, Scott V. (2017): Evaluating climate signal recorded in tree-ring δ13 C and δ18O values from bulk wood and α-cellulose for six species across four sites in the northeastern US. In *Rapid communications in mass spectrometry : RCM* 31 (24), pp. 2081–2091. DOI: 10.1002/rcm.7995.

Hanewinkel, Marc; Cullmann, Dominik A.; Schelhaas, Mart-Jan; Nabuurs, Gert-Jan; Zimmermann, Niklaus E. (2013): Climate change may cause severe loss in the economic value of European forest land. In *Nature Clim Change* 3 (3), pp. 203–207. DOI: 10.1038/NCLIMATE1687.

Harris, Ian; Osborn, Timothy J.; Jones, Phil; Lister, David (2020): Version 4 of the CRU TS monthly high-resolution gridded multivariate climate dataset. In *Scientific data* 7 (1), p. 109. DOI: 10.1038/s41597-020-0453-3.

Hartl-Meier, Claudia; Zang, Christian; Büntgen, Ulf; Esper, Jan; Rothe, Andreas; Göttlein, Axel et al. (2015): Uniform climate sensitivity in tree-ring stable isotopes across species and sites in a mid-latitude temperate forest. In *Tree physiology* 35 (1), pp. 4–15. DOI: 10.1093/treephys/tpu096.

Held, Isaac M.; Soden, Brian J. (2006): Robust responses of the hydrological cycle to global warming. In *Journal of climate* 19 (21), pp. 5686–5699.

Holmes, Richard L. (1983): Computer-assisted quality control in tree-ring dating and measurement.

IPCC (2019): Climate Change and Land: an IPCC Special Report on climate change, desertification, land degradation, sustainable land management, food security, and greenhouse gas fluxes in

terrestrial (Summary for Policymakers) ecosystems. Geneva, Switzerland: Intergovernmental Panel on Climate Change (IPCC).

Keel, Sonja G.; Joos, Fortunat; Spahni, Renato; Saurer, Matthias; Weigt, Rosemarie B.; Klesse, Stefan (2016): Simulating oxygen isotope ratios in tree ring cellulose using a dynamic global vegetation model. In *Biogeosciences* 13 (13), pp. 3869–3886. DOI: 10.5194/bg-13-3869-2016.

Keller, Kathrin M.; Lienert, Sebastian; Bozbiyik, Anil; Stocker, Thomas F.; Churakova, Olga V.; Frank, David C. et al. (2017): 20th century changes in carbon isotopes and water-use efficiency: tree-ring-based evaluation of the CLM4.5 and LPX-Bern models. In *Biogeosciences* 14 (10), pp. 2641–2673. DOI: 10.5194/bg-14-2641-2017.

Kirdyanov, Alexander V.; Treydte, Kerstin S.; Nikolaev, Anatolii; Helle, Gerhard; Schleser, Gerhard H. (2008): Climate signals in tree-ring width, density and δ13C from larches in Eastern Siberia (Russia). In *Chemical Geology* 252 (1-2), pp. 31–41. DOI: 10.1016/j.chemgeo.2008.01.023.

Klein, Tamir (2014): The variability of stomatal sensitivity to leaf water potential across tree species indicates a continuum between isohydric and anisohydric behaviours. In *Funct Ecol* 28 (6), pp. 1313–1320. DOI: 10.1111/1365-2435.12289.

Klesse, Stefan; DeRose, Robert Justin; Babst, Flurin; Black, Bryan A.; Anderegg, Leander D. L.; Axelson, Jodi et al. (2020): Continental-scale tree-ring-based projection of Douglas-fir growth: Testing the limits of space-for-time substitution. In *Global Change Biol*. DOI: 10.1111/gcb.15170.

Klesse, Stefan; Weigt, Rosemarie; Treydte, Kerstin S.; Saurer, Matthias; Schmid, Lola; Siegwolf, Rolf T.W.; Frank, David C. (2018): Oxygen isotopes in tree rings are less sensitive to changes in tree size and relative canopy position than carbon isotopes. In *Plant, cell & environment* 41 (12), pp. 2899–2914. DOI: 10.1111/pce.13424.

Kolář, Tomáš; Čermák, Petr; Trnka, Miroslav; Žid, Tomáš; Rybníček, Michal (2017): Temporal changes in the climate sensitivity of Norway spruce and European beech along an elevation gradient in Central Europe. In *Agricultural and Forest Meteorology* 239, pp. 24–33. DOI: 10.1016/j.agrformet.2017.02.028.

Krejza, Jan; Cienciala, Emil; Světlík, Jan; Bellan, Michal; Noyer, Estelle; Horáček, Petr et al. (2020): Evidence of climate-induced stress of Norway spruce along elevation gradient preceding the current dieback in Central Europe. In *Trees*. DOI: 10.1007/s00468-020-02022-6.

Labuhn, Inga; Daux, Valérie; Girardclos, Olivier; Stievenard, Michel; Pierre, Monique; Masson-Delmotte, Valérie (2016): French summer droughts since 1326 CE: a reconstruction based on tree ring cellulose δ18 O. In *Clim. Past* 12 (5), pp. 1101–1117. DOI: 10.5194/cp-12-1101-2016.

Labuhn, Inga; Daux, Valérie; Pierre, Monique; Stievenard, Michel; Girardclos, Olivier; Féron, Anaïs et al. (2014): Tree age, site and climate controls on tree ring cellulose δ18O: A case study on oak trees from south-western France. In *Dendrochronologia* 32 (1), pp. 78–89. DOI: 10.1016/j.dendro.2013.11.001.

Laumer, W.; Andreu, Laia; Helle, Gerd; Schleser, G. H.; Wieloch, T.; Wissel, H. (2009): A novel approach for the homogenization of cellulose to use micro-amounts for stable isotope analyses. In *Rapid communications in mass spectrometry: RCM* 23 (13), pp. 1934–1940. DOI: 10.1002/rcm.4105.

Leavitt, Steven W. (1993): Seasonal 13 C/ 12 C changes in tree rings: species and site coherence, and a possible drought influence. In *Can. J. For. Res.* 23 (2), pp. 210–218. DOI: 10.1139/x93-028.

Lehmann, Marco; Gamarra, Bruno; Kahmen, Ansgar; Siegwolf, Rolf T.W.; Saurer, Matthias (2017): Oxygen isotope fractionations across individual leaf carbohydrates in grass and tree species. In *Plant, cell & environment* 40 (8), pp. 1658–1670. DOI: 10.1111/pce.12974.

Lenth, Russell V. (2016): Least-Squares Means: The R Package lsmeans. In *Journal of Statistical Software* 69 (1), pp. 1–33. DOI: 10.18637/jss.v069.i01.

Leuenberger, Markus (2007): To What Extent Can Ice Core Data Contribute to the Understanding of Plant Ecological Developments of the Past? In : Stable Isotopes as Indicators of Ecological Change, vol. 1: Elsevier (Terrestrial Ecology), pp. 211–233.

Levesque, Mathieu; Andreu-Hayles, Laia; Pederson, Neil (2017): Water availability drives gas exchange and growth of trees in northeastern US, not elevated CO2 and reduced acid deposition. In *Scientific reports* 7, p. 46158. DOI: 10.1038/srep46158.

Levesque, Mathieu; Andreu-Hayles, Laia; Smith, William Kolby; Williams, A. Park; Hobi, Martina L.; Allred, Brady W.; Pederson, Neil (2019): Tree-ring isotopes capture interannual vegetation productivity dynamics at the biome scale. In *Nature communications* 10 (1), p. 742. DOI: 10.1038/s41467-019-08634-y.

Lévesque, Mathieu; Saurer, Matthias; Siegwolf, Rolf T.W.; Eilmann, Britta; Brang, Peter; Bugmann, Harald; Rigling, Andreas (2013): Drought response of five conifer species under contrasting water availability suggests high vulnerability of Norway spruce and European larch. In *Global Change Biol* 19 (10), pp. 3184–3199. DOI: 10.1111/gcb.12268.

Lindner, Marcus; Maroschek, Michael; Netherer, Sigrid; Kremer, Antoine; Barbati, Anna; Garcia-Gonzalo, Jordi et al. (2010): Climate change impacts, adaptive capacity, and vulnerability of European forest ecosystems. In *Forest Ecology and Management* 259 (4), pp. 698–709. DOI: 10.1016/j.foreco.2009.09.023.

Liu, Li-Min; Qi, Hua; Luo, Xin-Lan; Zhang, Xuan (2008): Coordination effect between vapor water loss through plant stomata and liquid water supply in soil-plant-atmosphere continuum (SPAC): a review. In *Ying yong sheng tai xue bao = The journal of applied ecology* 19 (9), pp. 2067–2073.

Liu, Xiaohong; An, Wenling; Leavitt, Steven W.; Wang, Wenzhi; Xu, Guobao; Zeng, Xiaomin; Qin, Dahe (2014): Recent strengthening of correlations between tree-ring δ13C and δ18O in mesic western China: Implications to climatic reconstruction and physiological responses. In *Global and Planetary Change* 113, pp. 23–33. DOI: 10.1016/j.gloplacha.2013.12.005.

Loader, Neil J.; McCarroll, Danny; Gagen, M. H.; Robertson, Iain; Jalkanen, Risto (2007): Extracting Climatic Information from Stable Isotopes in Tree Rings. In : Stable Isotopes as Indicators of Ecological Change, vol. 1: Elsevier (Terrestrial Ecology), pp. 25–48.

Loader, Neil J.; Young, Giles H. F.; McCarroll, Danny; Davies, Darren; Miles, Daniel; Bronk Ramsey, Christopher (2020): Summer precipitation for the England and Wales region, 1201–2000 ce, from stable oxygen isotopes in oak tree rings. In *J. Quaternary Sci.* 35 (6), pp. 731–736. DOI: 10.1002/jqs.3226.

Löw, M.; Herbinger, K.; Nunn, A. J.; Häberle, Karl-Heinz; Leuchner, M.; Heerdt, C. et al. (2006): Extraordinary drought of 2003 overrules ozone impact on adult beech trees (Fagus sylvatica). In *Trees* 20 (5), pp. 539–548. DOI: 10.1007/s00468-006-0069-z.

Lyr, Horst (Ed.) (1992): Physiologie und Ökologie der Gehölze. Mit 85 Tabellen. Jena: Fischer.

Maxwell, S. R.; Belmecheri, Soumaya; Taylor, Alan H.; Davis, Kenneth J.; Ocheltree, Troy W. (2020): Carbon isotope ratios in tree rings respond differently to climatic variations than tree-ring width in a mesic temperate forest. In *Agricultural and Forest Meteorology* 288-289, p. 108014. DOI: 10.1016/j.agrformet.2020.108014.

McCarroll, Danny; Loader, Neil J. (2004): Stable isotopes in tree rings. In *Quaternary Science Reviews* 23 (7-8), pp. 771–801. DOI: 10.1016/j.quascirev.2003.06.017.

McDowell, Nate; Pockman, William T.; Allen, Craig D.; Breshears, David D.; Cobb, Neil; Kolb, Thomas et al. (2008): Mechanisms of plant survival and mortality during drought: why do some plants survive while others succumb to drought? In *The New phytologist* 178 (4), pp. 719–739. DOI: 10.1111/j.1469-8137.2008.02436.x.

McDowell, Nate G.; Beerling, David J.; Breshears, David D.; Fisher, Rosie A.; Raffa, Kenneth F.; Stitt, Mark (2011a): The interdependence of mechanisms underlying climate-driven vegetation

mortality. In *Trends in ecology & evolution* 26 (10), pp. 523–532. DOI: 10.1016/j.tree.2011.06.003.

McDowell, Nate G.; Bond, Barbara J.; Dickman, Lee T.; Ryan, Michael G.; Whitehead, David (2011b): Relationships Between Tree Height and Carbon Isotope Discrimination. In F. C. Meinzer, Barbara Lachenbruch, Todd E. Dawson (Eds.): Size- and age-related changes in tree structure and function, vol. 4. Dordrecht, London: Springer (Tree Physiology, v. 4), pp. 255–286.

Mölder, Inga; Leuschner, Christoph; Leuschner, Hanns Hubert (2011): δ13C signature of tree rings and radial increment of Fagus sylvatica trees as dependent on tree neighborhood and climate. In *Trees* 25 (2), pp. 215–229. DOI: 10.1007/s00468-010-0499-5.

O'Reilly Sternberg, Leonel da Silveira Lobo (2009): Oxygen stable isotope ratios of tree-ring cellulose: the next phase of understanding. In *The New phytologist* 181 (3), pp. 553–562. DOI: 10.1111/j.1469-8137.2008.02661.x.

Peñuelas, Josep; Hunt, Jenny M.; Ogaya, Romà; Jump, Alistar S. (2008): Twentieth century changes of tree-ring δ 13 C at the southern range-edge of Fagus sylvatica: increasing water-use efficiency does not avoid the growth decline induced by warming at low altitudes. In *Global Change Biol* 14 (5), pp. 1076–1088. DOI: 10.1111/j.1365-2486.2008.01563.x.

Piovesan, G.; Biondi, Franco; Di Filippo, A.; Alessandrini, A.; Maugeri, M. (2008): Drought-driven growth reduction in old beech (Fagus sylvatica L.) forests of the central Apennines, Italy. Global Change Biology, 14(6), 1265-1281. In *Global Change Biol* 14 (6), pp. 1265–1281. DOI: 10.1111/J.1365-2486.2008.01570.X.

Pretzsch, H.; Schütze, G.; Uhl, E. (2013): Resistance of European tree species to drought stress in mixed versus pure forests: evidence of stress release by inter-specific facilitation. In *Plant biology (Stuttgart, Germany)* 15 (3), pp. 483–495. DOI: 10.1111/j.1438-8677.2012.00670.x.

R Core Team (2020): R: A language and environment for statistical computing. In *R Foundation for Statistical Computing, Vienna, Austria.* Available online at URL https://www.R-project.org/.

Rezaie, Negar; D'Andrea, Ettore; Bräuning, Achim; Matteucci, Giorgio; Bombi, Pierluigi; Lauteri, Marco (2018): Do atmospheric CO2 concentration increase, climate and forest management affect iWUE of common beech? Evidences from carbon isotope analyses in tree rings. In *Tree physiology* 38 (8), pp. 1110–1126. DOI: 10.1093/treephys/tpy025.

Rinne, K. T.; Loader, Neil J.; Switsur, Vincent R.; Waterhouse, J. S. (2013): 400-year May–August precipitation reconstruction for Southern England using oxygen isotopes in tree rings. In *Quaternary Science Reviews* 60, pp. 13–25. DOI: 10.1016/j.quascirev.2012.10.048.

Roden, John S.; Lin, Guanghui; Ehleringer, James R. (2000): A mechanistic model for interpretation of hydrogen and oxygen isotope ratios in tree-ring cellulose. In *Geochimica et Cosmochimica Acta* 64 (1), pp. 21–35. DOI: 10.1016/S0016-7037(99)00195-7.

Roden, John S.; Siegwolf, Rolf T.W. (2012): Is the dual-isotope conceptual model fully operational? In *Tree physiology* 32 (10), pp. 1179–1182. DOI: 10.1093/treephys/tps099.

Salmon, Yann; Lintunen, Anna; Dayet, Alexia; Chan, Tommy; Dewar, Roderick; Vesala, Timo; Hölttä, Teemu (2020): Leaf carbon and water status control stomatal and nonstomatal limitations of photosynthesis in trees. In *The New phytologist* 226 (3), pp. 690–703. DOI: 10.1111/nph.16436.

Saurer, M.; Aellen K.; Siegwolf, Rolf T.W. (1997): Correlating delta13C and delta18O in cellulose of trees. In *Plant Cell Environ* 20 (12), pp. 1543–1550. DOI: 10.1046/j.1365-3040.1997.d01-53.x.

Saurer, M.; Cherubini, P.; Reynolds-Henne, C. E.; Treydte, Kerstin S.; Anderson, W. T.; Siegwolf, Rolf T.W. (2008): An investigation of the common signal in tree ring stable isotope chronologies at temperate sites. In *J. Geophys. Res.* 113 (G4), 31,625. DOI: 10.1029/2008JG000689.

Saurer, M.; Siegenthaler, U.; Schweingruber, Fritz H. (1995): The climate-carbon isotope relationship in tree rings and the significance of site conditions. In *Tellus B* 47 (3), pp. 320–330. DOI: 10.1034/j.1600-0889.47.issue3.4.x.

Saurer, Matthias; Kress, Anne; Leuenberger, Markus; Rinne, Katja T.; Treydte, Kerstin S.; Siegwolf, Rolf T.W. (2012): Influence of atmospheric circulation patterns on the oxygen isotope ratio of tree rings in the Alpine region. In *J. Geophys. Res.* 117 (D5), 12. DOI: 10.1029/2011JD016861.

Saurer, Matthias; Spahni, Renato; Frank, David C.; Joos, Fortunat; Leuenberger, Markus; Loader, Neil J. et al. (2014): Spatial variability and temporal trends in water-use efficiency of European forests. In *Global Change Biol* 20 (12), pp. 3700–3712. DOI: 10.1111/gcb.12717.

Schäfer, Cynthia; Grams, Thorsten; Rötzer, Thomas; Feldermann, Aline; Pretzsch, Hans (2017): Drought Stress Reaction of Growth and Δ13C in Tree Rings of European Beech and Norway Spruce in Monospecific Versus Mixed Stands Along a Precipitation Gradient. In *Forests* 8 (6), p. 177. DOI: 10.3390/f8060177.

Scheidegger, Y.; Saurer, M.; Bahn, M.; Siegwolf, Rolf T.W. (2000): Linking stable oxygen and carbon isotopes with stomatal conductance and photosynthetic capacity: a conceptual model. In *Oecologia* 125 (3), pp. 350–357. DOI: 10.1007/S004420000466.

Schleser, Gerhard H.; Helle, Gerhard; Lücke, Andreas; Vos, Heinz (1999): Isotope signals as climate proxies: the role of transfer functions in the study of terrestrial archives. In *Quaternary Science Reviews* 18 (7), pp. 927–943. DOI: 10.1016/S0277-3791(99)00006-2.

Schuldt, Bernhard; Buras, Allan; Arend, Matthias; Vitasse, Yann; Beierkuhnlein, Carl; Damm, Alexander et al. (2020): A first assessment of the impact of the extreme 2018 summer drought on Central European forests. In *Basic and Applied Ecology* 45, pp. 86–103. DOI: 10.1016/j.baae.2020.04.003.

Schweingruber, Fritz H. (1976): Tree Rings and Climate. Oxford: Elsevier Science. Available online at http://site.ebrary.com/lib/alltitles/docDetail.action?docID=10685739.

Shestakova, Tatiana A.; Voltas, Jordi; Saurer, Matthias; Berninger, Frank; Esper, Jan; Andreu-Hayles, Laia et al. (2019): Spatio-temporal patterns of tree growth as related to carbon isotope fractionation in European forests under changing climate. In *Global Ecol Biogeogr* 28 (9), pp. 1295–1309. DOI: 10.1111/geb.12933.

Soh, Wuu Kuang; Yiotis, Charilaos; Murray, Michelle; Parnell, Andrew; Wright, Ian J.; Spicer, Robert A. et al. (2019): Rising CO2 drives divergence in water use efficiency of evergreen and deciduous plants. In *Science advances* 5 (12), eaax7906. DOI: 10.1126/sciadv.aax7906.

Szejner, Paul; Wright, William E.; Babst, Flurin; Belmecheri, Soumaya; Trouet, Valerie; Leavitt, Steven W. et al. (2016): Latitudinal gradients in tree ring stable carbon and oxygen isotopes reveal differential climate influences of the North American Monsoon System. In *J. Geophys. Res.* 121 (7), pp. 1978–1991. DOI: 10.1002/2016JG003460.

Treydte, Kerstin S.; Boda, Sonja; Graf Pannatier, Elisabeth; Fonti, Patrick; Frank, David C.; Ullrich, Bastian et al. (2014): Seasonal transfer of oxygen isotopes from precipitation and soil to the tree ring: source water versus needle water enrichment. In *The New phytologist* 202 (3), pp. 772–783. DOI: 10.1111/nph.12741.

Treydte, Kerstin S.; Frank, David C.; Esper, Jan; Andreu, Laia; Bednarz, Zdzisław; Berninger, Frank et al. (2007): Signal strength and climate calibration of a European tree-ring isotope network. In *Geophys. Res. Lett.* 34 (24), p. 224. DOI: 10.1029/2007GL031106.

Treydte, Kerstin S.; Schleser, Gerhard H.; Helle, Gerhard; Frank, David C.; Winiger, Matthias; Haug, Gerald H.; Esper, Jan (2006): The twentieth century was the wettest period in northern Pakistan over the past millennium. In *Nature* 440 (7088), pp. 1179–1182. DOI: 10.1038/nature04743.

Treydte, Kerstin S.; Schleser, Gerhard H.; Schweingruber, Fritz H.; Winiger, Matthias (2001): The climatic significance of δ 13 C in subalpine spruces (Lötschental, Swiss Alps). In *Tellus B: Chemical and Physical Meteorology* 53 (5), pp. 593–611. DOI: 10.3402/tellusb.v53i5.16639.

van der Maaten, Ernst (2012): Climate sensitivity of radial growth in European beech (Fagus sylvatica L.) at different aspects in southwestern Germany. In *Trees* 26 (3), pp. 777–788. DOI: 10.1007/s00468-011-0645-8.

van Mantgem, Phillip J.; Stephenson, Nathan L.; Byrne, John C.; Daniels, Lori D.; Franklin, Jerry F.; Fulé, Peter Z. et al. (2009): Widespread increase of tree mortality rates in the western United States. In *Science (New York, N.Y.)* 323 (5913), pp. 521–524. DOI: 10.1126/science.1165000.

Vicente-Serrano, Sergio M.; Beguería, Santiago; López-Moreno, Juan I. (2010): A Multiscalar Drought Index Sensitive to Global Warming: The Standardized Precipitation Evapotranspiration Index. In *Journal of climate* 23 (7), pp. 1696–1718. DOI: 10.1175/2009JCLI2909.1.

Vitali, Valentina; Büntgen, Ulf; Bauhus, Jürgen (2017): Silver fir and Douglas fir are more tolerant to extreme droughts than Norway spruce in south-western Germany. In *Global Change Biol* 23 (12), pp. 5108–5119. DOI: 10.1111/gcb.13774.

Vitali, Valentina; Forrester, David I.; Bauhus, Jürgen (2018): Know Your Neighbours: Drought Response of Norway Spruce, Silver Fir and Douglas Fir in Mixed Forests Depends on Species Identity and Diversity of Tree Neighbourhoods. In *Ecosystems* 21 (6), pp. 1215–1229. DOI: 10.1007/s10021-017-0214-0.

Vitasse, Yann; Bottero, Alessandra; Cailleret, Maxime; Bigler, Christof; Fonti, Patrick; Gessler, Arthur et al. (2019): Contrasting resistance and resilience to extreme drought and late spring frost in five major European tree species. In *Global Change Biol* 25 (11), pp. 3781–3792. DOI: 10.1111/gcb.14803.

Volkmann, Till H. M.; Haberer, Kristine; Gessler, Arthur; Weiler, Markus (2016): High-resolution isotope measurements resolve rapid ecohydrological dynamics at the soil-plant interface. In *The New phytologist* 210 (3), pp. 839–849. DOI: 10.1111/nph.13868.

Walthert, Lorenz; Ganthaler, Andrea; Mayr, Stefan; Saurer, Matthias; Waldner, Peter; Walser, Marco et al. (2020): From the comfort zone to crown dieback: Sequence of physiological stress thresholds in mature European beech trees across progressive drought. In *Science of The Total Environment*, p. 141792. DOI: 10.1016/j.scitotenv.2020.141792.

Weigt, Rosemarie B.; Bräunlich, Stephanie; Zimmermann, Lothar; Saurer, Matthias; Grams, Thorsten E.E.; Dietrich, Hans-Peter et al. (2015): Comparison of δ18O and δ13C values between tree-ring whole wood and cellulose in five species growing under two different site conditions. In *Rapid communications in mass spectrometry: RCM* 29 (23), pp. 2233–2244. DOI: 10.1002/rcm.7388.

Weigt, Rosemarie B.; Streit, Kathrin; Saurer, Matthias; Siegwolf, Rolf T.W. (2018): The influence of increasing temperature and CO2 concentration on recent growth of old-growth larch: contrasting responses at leaf and stem processes derived from tree-ring width and stable isotopes. In *Tree physiology* 38 (5), pp. 706–720. DOI: 10.1093/treephys/tpx148.

Will, Rodney E.; Wilson, Stuart M.; Zou, Chris B.; Hennessey, Thomas C. (2013): Increased vapor pressure deficit due to higher temperature leads to greater transpiration and faster mortality during drought for tree seedlings common to the forest-grassland ecotone. In *The New phytologist* 200 (2), pp. 366–374. DOI: 10.1111/nph.12321.

Williams, P. A.; Allen, Craig D.; Macalady, Alison K.; Griffin, Daniel; Woodhouse, Connie A.; Meko, David M. et al. (2013): Temperature as a potent driver of regional forest drought stress and tree mortality. In *Nature Clim Change* 3 (3), pp. 292–297. DOI: 10.1038/nclimate1693.

Woodley, E. J.; Loader, Neil J.; d. McCarroll; Young, G.H.F.; Robertson, I.; Heaton, T.H.E.; Gagen, M. H. (2012): Estimating uncertainty in pooled stable isotope time-series from tree-rings. In *Chemical Geology* 294-295, pp. 243–248. DOI: 10.1016/j.chemgeo.2011.12.008.

Zang, Christian (2011): Growth Reaction of Temperate Forest Trees to Summer Drought: A Multispecies Tree-ring Network Approach. TU München, München. Available online at https://books.google.ch/books?id=tpFvmgEACAAJ.

Zang, Christian; Biondi, Franco (2015): treeclim: an R package for the numerical calibration of proxy-climate relationships. In *Ecography* 38 (4), pp. 431–436. DOI: 10.1111/ecog.01335.

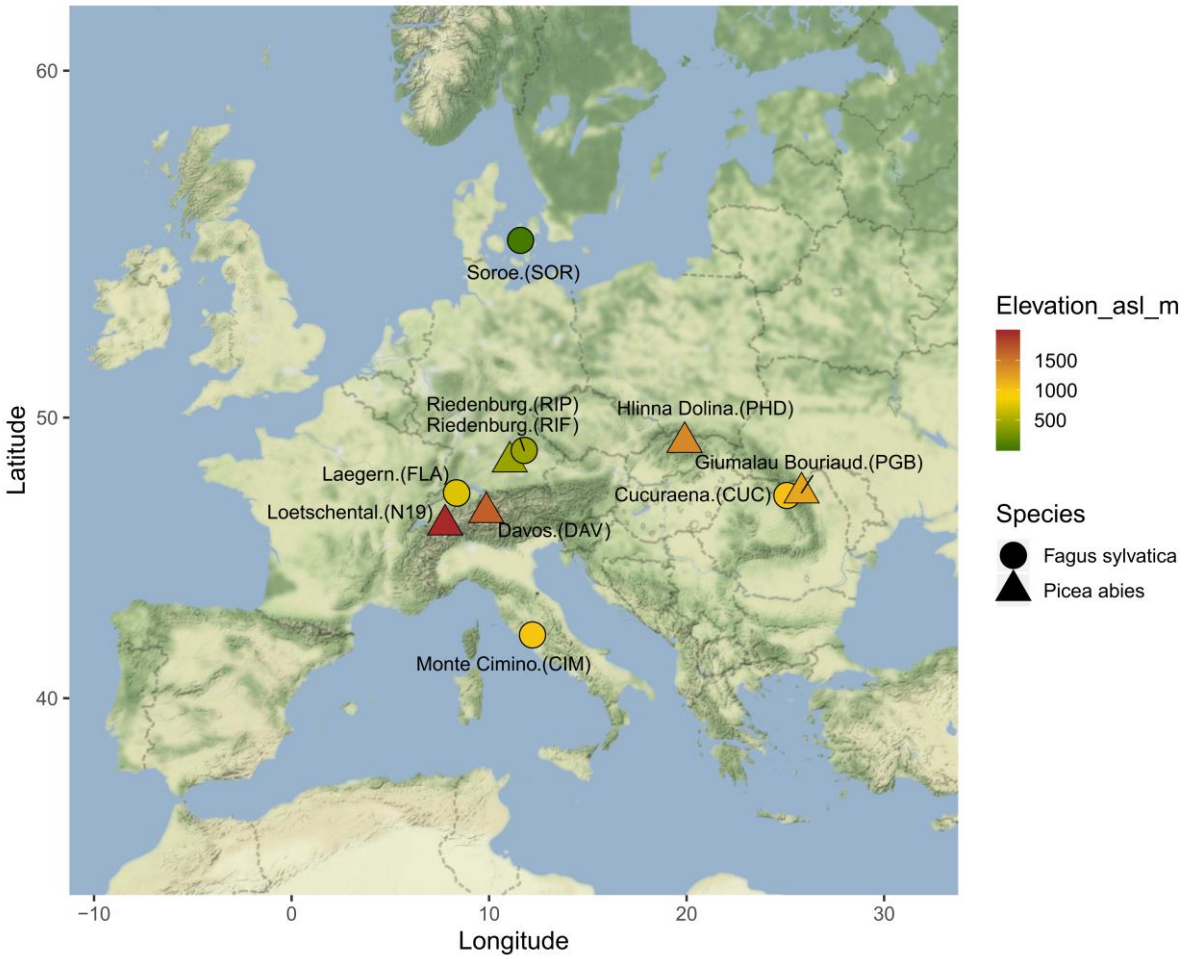

Fig. 1 Location of the study sites. Different shapes describe species sampled at each site, and site elevation is indicated by the symbol colour.

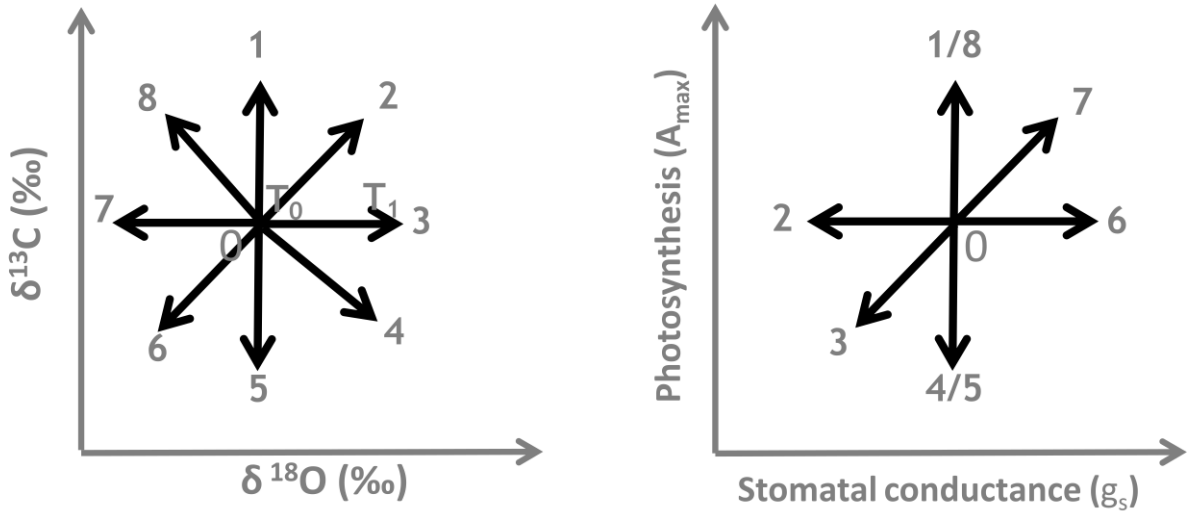

Fig. 2 Conceptual application of the Scheidegger model (adapted from Scheidegger et al. 2000), showing the possible scenarios in $\delta^{13}C$ and $\delta^{18}O$ and respective changes in A_{net} and g_s (1-8). T_0 indicates the average isotope values of the first time window, and T_1 indicates the averages from the second time window.

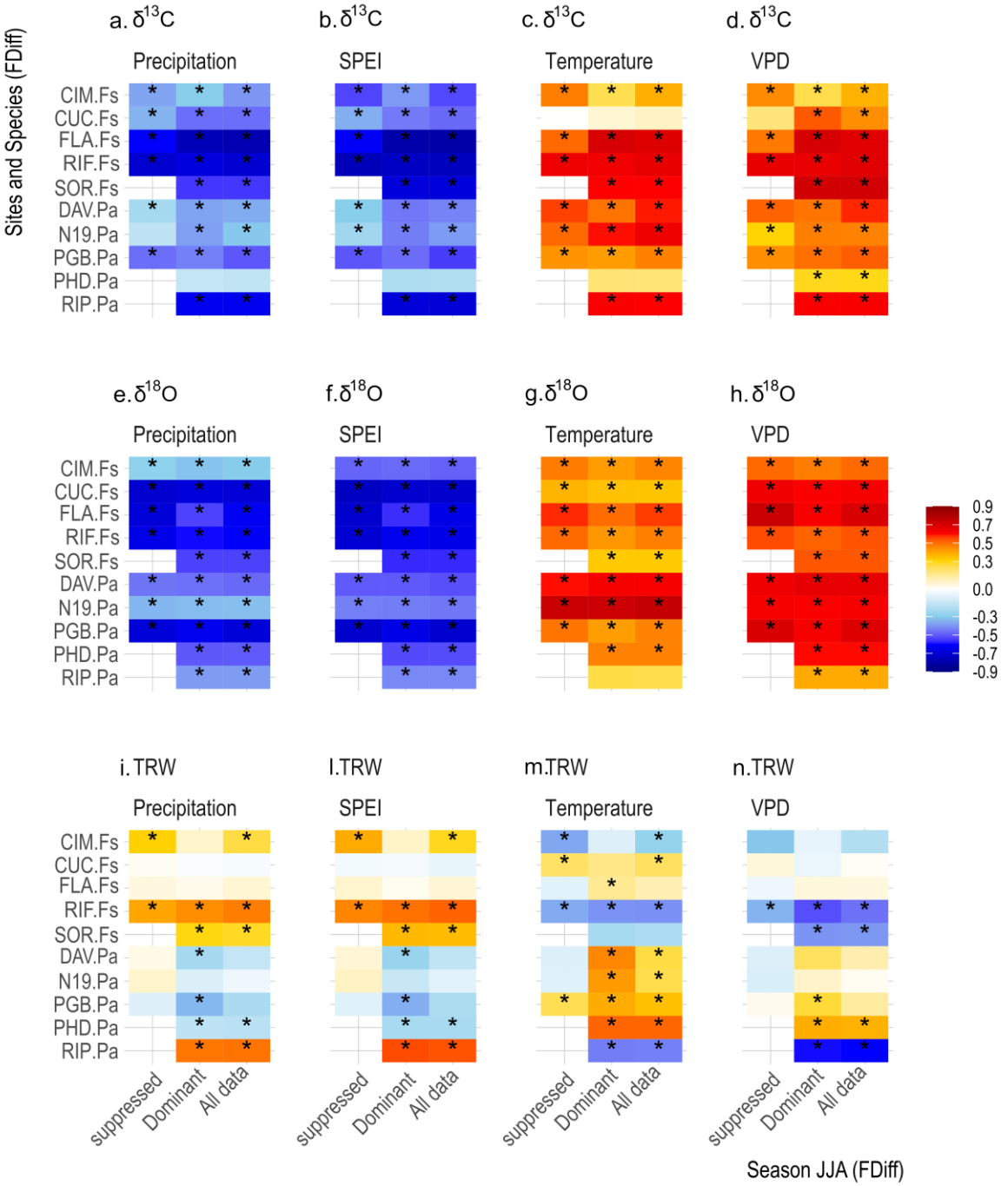

Fig. 3 Pearson's correlation coefficients calculated between FDiff $\delta^{13}C$ (upper panels a-d), FDiff $\delta^{18}O$ (middle panels, e-h) and FDiff TRW on one side (lower panels, i-n) and FDiff climate parameters of summer (JJA) precipitation, SPEI, temperature and VPD on the other side. Correlations span the 1935-2012 common period, and are separated for suppressed and

dominant trees, and finally calculated for the whole dataset for each site. Significant correlations are indicated by asterisks (p<0.05=*).

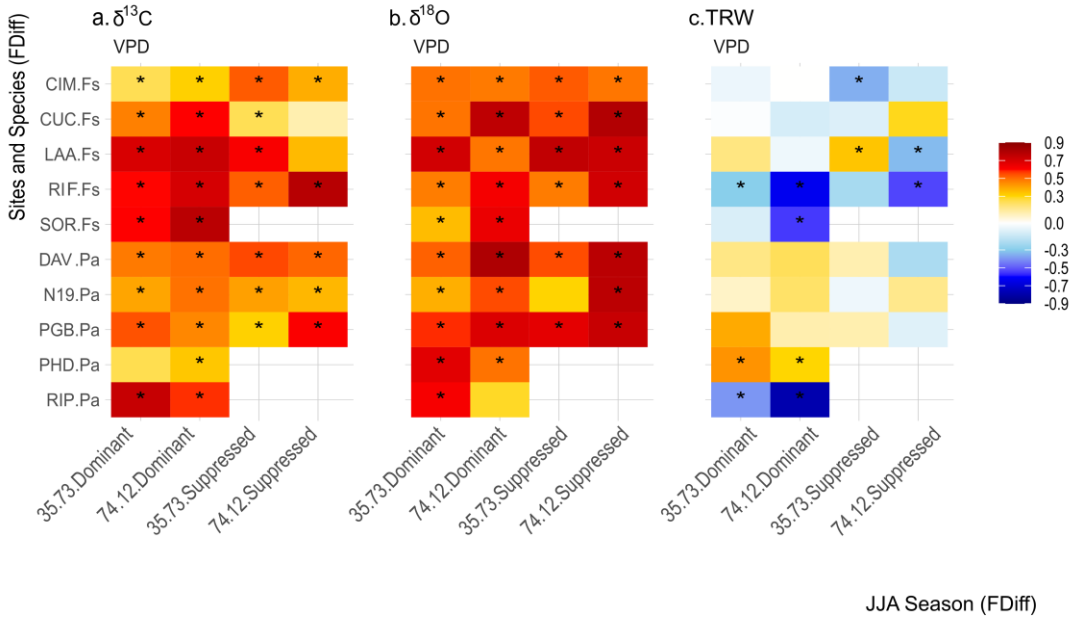

Fig. 4 Pearson's correlation coefficients calculated between FDiff δ13C (a), FDiff δ18O (b) and FDiff TRW on one side (c) and FDiff VPD of summer (JJA) on the other side, for the two time windows (1935-1973 and 1974-2012), and separated for dominant and suppressed trees. Significant correlations are indicated by the asterisk (p<0.05=*).

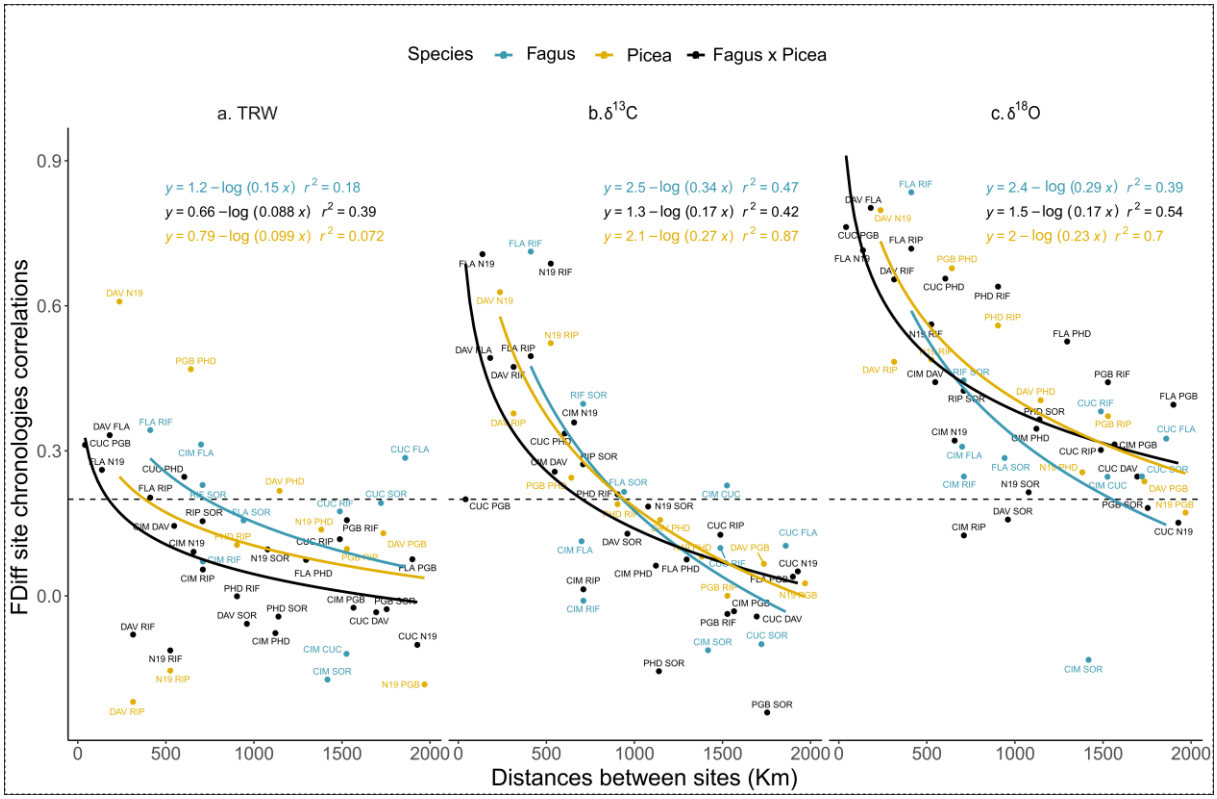

Fig. 5 Between-sites correlation of FDiff TRW (a), $\delta^{13}C$ (b) and $\delta^{18}O$ (c) chronologies for the common period (1935-20112). Distances between sites are indicated in km. Model lines are fitted

as y=log(x). Dashed horizontal line indicates r= p<0.05. Each analysis was done separately for beech, spruce, and their combination (black line).

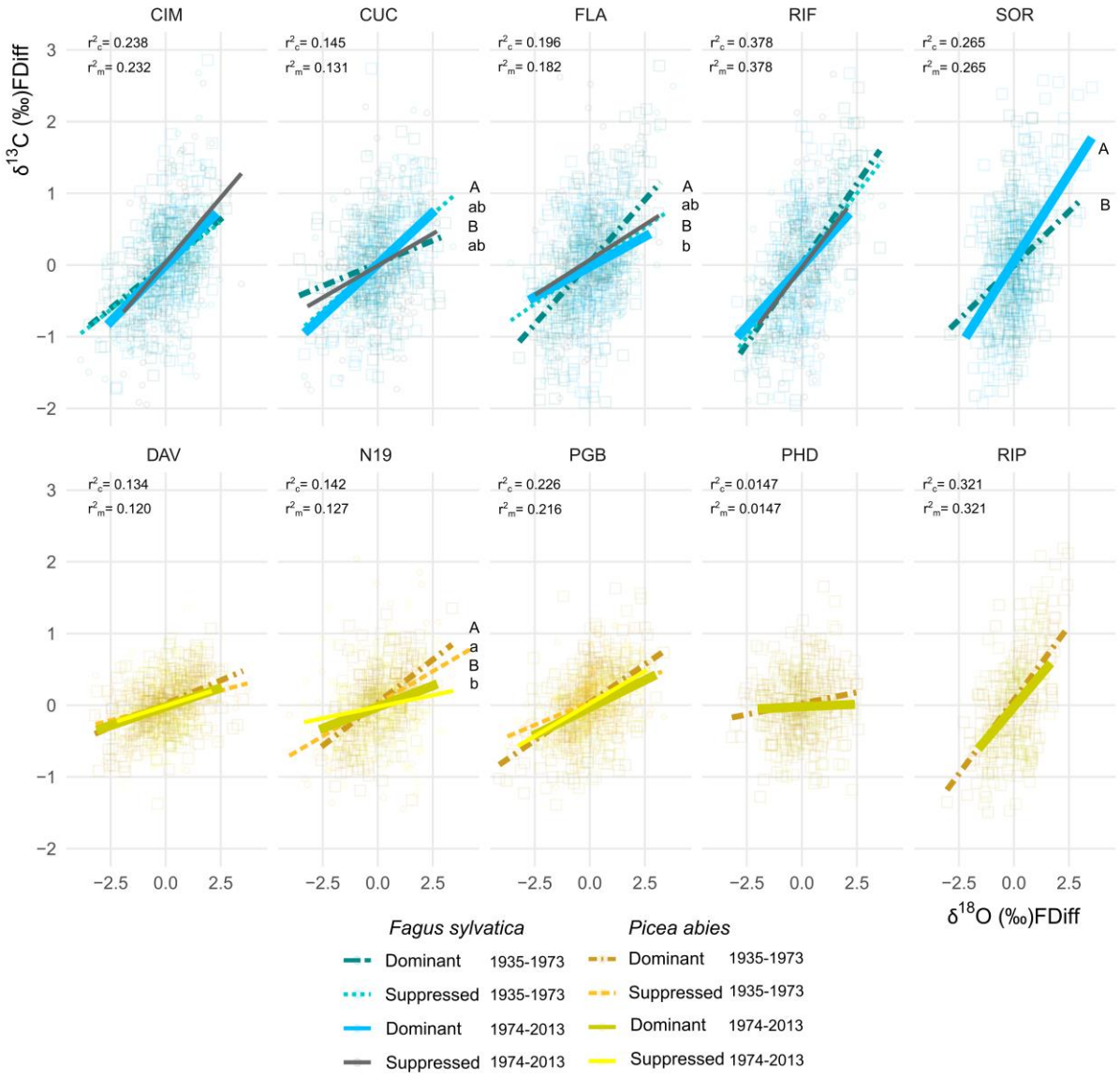

Fig. 6 Relationships between $\delta^{13}C$ and $\delta^{18}O$ FDiff across all sites, for dominant and suppressed species and two time periods. Significant differences in the slopes are indicated by different letters. No letters indicate non-significant differences in the slopes across all four groups. Dominant trees are indicated by capital letters, while minuscule lettering indicates the group of suppressed trees, e.g., "a" and "A" are statistically the same. The order of the groups follows the ordering of the legend. Conditional r^2 (r^2_c) and marginal r^2 (r^2_m) are indicated for each model.

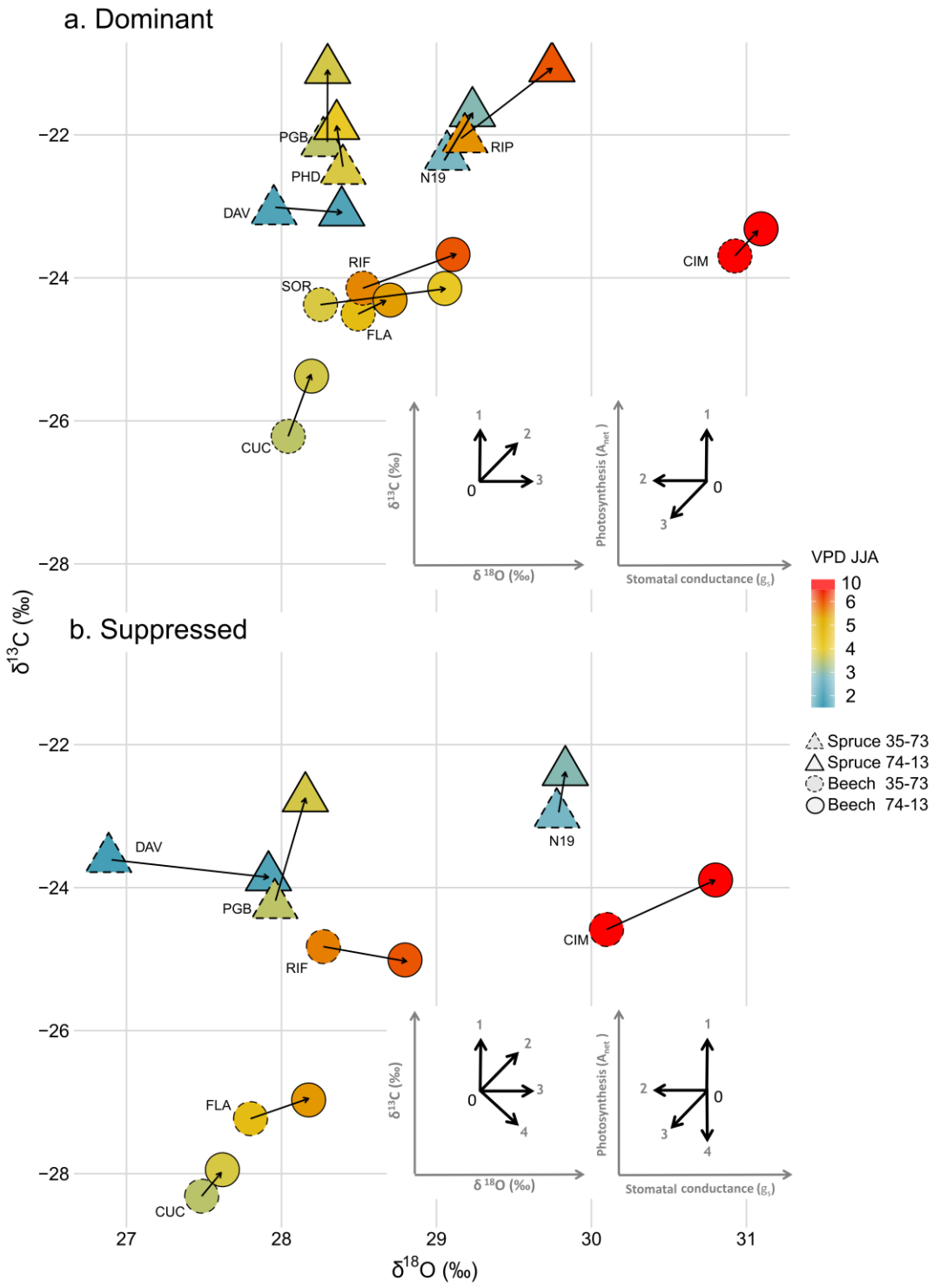

Fig. 3 Shift in mean isotope values per site and canopy layers between the two distinguished time periods 1935-1973 (dashed line) and 1973-2012 (solid line), and the two species (spruce: triangle; beech: circle). Arrows indicate significant changes in the raw values of $\delta^{13}C$ and/or $\delta^{18}O$ at $p<0.05$. Direction of shift corresponds to changes in photosynthesis (A_{net}) and stomatal conductance (g_s) according to the dual isotope model after Scheidegger et al. (2000), as depicted in the lower panel. Colouring indicates mean June-August VPD (hPa) from low VPD (blue), over intermediate (green/yellow), to high VPD (red).

Table 1 Geographic and climatic characteristics of the sites. Climatic variables represent the averages means for the common study period (i.e. 1935-2012), with T= mean annual temperature, P =mean annual precipitation sum, VPD = average mean vapour pressure deficit for the summer months of June, July and August (JJA). The sample number for each site is indicated by number of dominant and supressed trees. The references where each site information were firstly published are coded as follows: K16= (Keel et al. 2016), K17= (Keller et al. 2017), K18= (Klesse et al. 2018).

Site	ID	Species	Coord. N	Coord. E	Elevation m a.s.l.	T [°C]	P [mm/yr]	VPD_JJA [kPa]	Dominant /suppressed trees	Previously published in
Monte Cimino	CIM	*Fagus sylvatica*	42,41	12,2	1008	11	711	10.6	5 / 5	K17 / K18
Cucuraena	CUC	*Fagus sylvatica*	47,4	25,08	1033	5,33	790	3.6	5 / 5	K17 / K18
Davos	DAV	*Picea abies*	46,82	9,86	1660	3,47	1004	1.8	5 / 5	K16 / K17 / K18
Giumalau Bouriaud	PGB	*Picea abies*	47,45	25,45	1200	3,98	848	3.6	5 / 7	K17 / K18
Hlinna Dolina	PHD	*Picea abies*	49,19	19,9	1400	2,55	1292	3.9	5 / 0	K17
Laegern	FLA	*Fagus sylvatica*	47,48	8,37	709	8,49	1129	5.1	7 / 6	K16 / K17 / K18
Loetschental	N19	*Picea abies*	46,39	7,77	1966	1,33	1716	2.7	4 / 7	K16 / K17 / K18
Riedenburg	RIF	*Fagus sylvatica*	48,92	11,78	430	8	732	5.8	5 / 5	K18
Riedenburg	RIP	*Picea abies*	48,92	11,78	430	8	732	5.8	5 / 0	K18
Soroe	SOR	*Fagus sylvatica*	55,42	11,59	35	8,28	595	4.0	7 / 0	unpublished